PB-214 990

CATIONIC POLYMERS AS FLOCCULANT AIDE IN WATER PURIFICATION

H. Linford, et al

Columbia University
New York, New York

1968

DISTRIBUTED BY:

NTIS

National Technical Information Service
U. S. DEPARTMENT OF COMMERCE
5285 Port Royal Road, Springfield Va. 22151

WP00240-06

Cmin.

PB 214 990

RECEIVED
LIBRARY

AUG 27 1968

FWPCA, OHIO BASIN REGION
4676 COLUMBIA PKWY., CINN., O

Reproduced by
NATIONAL TECHNICAL
INFORMATION SERVICE
U.S. Department of Commerce
Springfield VA 22151

Cationic Polymers as Flocculant Aids In Water Purification

H. Linford, R. Fyfe, W. Hilborn
and S. Lausangngam

The Department of Chemical Engineering
Columbia University

U. S. Public Health Service
Terminal Progress Report
WP 00240-06
1968

I. Introduction

According to some investigators (1-7), the flocculation mechanism is based on action of chemical bonding forces. Polymeric segments of a flocculant are adsorbed from the liquid phase onto the solid surface. Subsequently or simultaneously polymeric "bridging" occurs by means of multi-segment adsorption and polymeric crosslinking. The resulting flocs were thought to overcome the inertial and electrostatic repulsive forces which keep the unflocculated particles in suspension. These workers placed little emphasis on the possibility that the flocculant might alter the make-up of the double layer (a charge discontinuity which exists at phase boundaries) thereby reducing electrostatic repulsive forces between particles and flocs. The total mechanism is probably a combination of double layer makeup change and "bridging".

Behavior of the calculated electrokinetic or "Zeta" potential reflects change in the stability of a suspension. Stability depends on the electrostatic repulsive forces between suspended particles. It therefore depends on their net effective surface charge density. Collision probability depends on both normal Brownian movement and electrostatic repulsion. Reduction of surface charge density then increases collision probability. Flocculation depends on particle collisions. Flocculation behavior can therefore be correlated with Zeta potential.

One means of estimating the Zeta potential is from microelectrophoresis measurements. Previous investigators in this laboratory have shown that a zero value of electrophoretic mobility (the measured linear velocity of a suspended solid particle under the influence of a unit electrical potential gradient) approximately corresponds to optimum flocculation conditions. Flocculation effectiveness was evaluated by refiltration rate studies (the rate at which clear filtrate passes through a filter bed under constant vacuum conditions). The measurements were carried out for crystalline silica suspended in 10^{-3} N NaCl. The flocculant was a polyethyleneimine (a cationic polyelectrolyte) (8).

The same workers have shown that the average effective particle size is a maximum when refiltration rate is a maximum, i.e. at optimum flocculation conditions(9). The solid silica particles were polydispense (i.e. there was a wide variation in size). The settling of larger particle sizes had a noticable effect on electrophoretic mobility measurements. In fact, electrophoretic mobility appeared to be a function of percent solids settled. Andreasen pipette samples were used in order to consider the various percentages of settling. Human tendency is to track one particle size in preference to others. All of these facts cast doubt on the results of electrophoretic mobility measurements in regard to being representative of a flocculation system(10). It seems that the Zeta potential should

really be calculated as a weighted mean electrophoretic mobility based on all particles in a suspension.

The literature gives references (11-12) to use of Zeta potential, calculated from electrophoretic mobility measurements, as the control factor in flocculation and coagulation processes, such as are used to clarify industrial waste waters by removal of suspended solids. In view of the literature and the above mentioned results from this laboratory, streaming potential measurements have been considered (13). To obtain values of Zeta potential more representative of a given system, a specially modified streaming potential cell and apparatus were constructed (14) so that streaming potential measurements can be made on a porous plug formed as a bed of flocs by filtration of a given flocculated suspension. Streaming potential is the potential difference formed between the two ends of the porous plug when clear filtrate is forced by a known pressure drop to flow through the plug. Since the bed contains all the solids of the flocculation system, then the Zeta potential, calculated from streaming potential data, should in fact be representative of the entire system. Human bias is also eliminated. A comparison of results in this laboratory from both electrophoretic mobility and streaming potential measurements on identical flocculation systems has shown that there exists a wide discrepancy between the calculated Zeta potentials. For 0.04 wt% primary silica suspended in 10^{-3} N NaCl to which a known amount of flocculant (a polyethyleneimine) was added, the value of the Zeta

potential calculated from streaming potential data was about 2/3 of the value calculated from electrophoretic mobility data (15).

It has often been noted in the literature that when using streaming medium of extremely low specific conductivity (e.g. 10^{-6} mho/cm), the "apparent" value of Zeta potential calculated from streaming potential data is in error, since the properties of the liquid phase in the "capillaries" of the bed are not the same as the bulk properties (16). These liquid properties are the viscosity, the dielectric constant, and the specific conductivity. Bulk values for viscosity and dielectric constant have been shown to usually introduce only minor error (17,18). But the specific conductivity (the electrical conductance of a unit cube of liquid electrolyte) of the liquid phase must be the effective value existing in the "capillaries". When the bulk value of specific conductivity, λ, (measured outside the plug) is sufficiently high, the value, λ_c, existing for the liquid in the plug may be approximated by this bulk value. However, when this is not the case, some way must be devised to find the "capillary" effective value, λ_c.

The physical reason for the difference of λ_c from λ is the nature of the solid-liquid interfacial region. When dealing with a charged solid surface and an electrolytic liquid phase, a double layer (charge discontinuity) forms at or near the interface. The presence of excess ions and dipolar molecules in this region increases the effective specific conduc-

tivity of the liquid in the "capillaries". Since the discrepancy between λ_c and λ is due to excess conduction at or near the phase boundary, it has commonly been called surface conduction.

It is sometimes not feasible to use high electrolyte content so as to be able to approximate λ_c by λ. For example, consider potable water clarification. It was therefore proposed to study flocculation behavior (flocculation effectiveness being represented by refiltration rate measurements) in relation to the Zeta potential calculated from streaming potential data. Potable water (19) ranges from 0 to about 10^{-2} N in bulk electrolyte content expressed as NaCl or KCl. Therefore three levels of KCl concentration were chosen: 10^{-4} N, 10^{-3} N and 10^{-2} N. 10^{-4} N KCl was a lower limit due to the use of Ag,AgCl electrodes in the streaming potential cell. NaCl was not used due to the adverse effect of the Na ion on organic adsorption onto silica surfaces (20).

Studies were made of flocculation of dilute-electrolyte aqueous silica suspensions using a cationic polyelectrolytic polymer (i.e. a polethyleneimine) as the flocculant. For a series of systems indexed by various initial flocculant concentrations, both refiltration rates and streaming potential measurements were made. This series was repeated at the mentioned three levels of KCl concentration, thereby covering the use of streaming potential data for control over a large range of possible potable water systems.

Results show that, by measuring the floc bed depth and total electrical resistance of the streaming potential cell, as well as the streaming potential and its corresponding pressure difference driving force, a control factor, valid over the potable water range, can be calculated for each flocculation system investigated. This control factor EKCF is calculated from the easily obtained laboratory data just stated above, and EKCF behaves the same as Zeta potential with respect to suspension stability and with respect to optimum flocculation conditions. Analysis of data also gives evidence that the effect of surface conduction is reduced by increasing amounts of added flocculant.

II. Literature Survey

A. Flocculation of solids from aqueous suspension

1. Coagulation and flocculation

Consider an aqueous suspension of an electrostatically charged solid particulate material. Coagulation may be defined as the reduction of the electrostatic repulsive forces between particles, which results in the adherance of particles, which results in the adherance of particles to one another upon collision. The subsequent larger particle size then allows separation of the solid and liquid phases of the suspension. Additives which bring about coagulation are often ionic or polar in nature. Multivalency and polarity of an additive molecule can improve coagulation since several primary suspension particles may be attracted to a single additive moelcule. Usually physical bonding forces are active between the additive coagulant and the primary solid particles.

Some authors separately define the term flocculation as a special case of coagulation, where bonding between primary solid particles and the "flocculant" is nearer chemical than physical (21). Flocculation involves a combination of physical and/or chemical adsorption of the flocculant onto the surface of the primary solid, followed by "bridging" between the primary particles. Bridging is caused by multi-site adsorption of the flocculant and by crosslinking via chemical, or hydrogen, bonding between adsorbed flocculant molecules.

2. The eighth power law

Smellie, La Mer et al (22-28) describe studies of subsidence, flocculation and refiltration of phosphate slimes. They placed emphasis on testing a variety of flocculants, including cationic, anionic and non-ionic polymeric materials. An optimum concentration of flocculant, corresponding to a maximum rate of refiltration, was noted. Effectiveness of flocculation was shown to be function of flocculant concentration, slime composition, weight percent of primary solid material, primary particle size, pH and extraneous electrolyte content. Noting that refiltration rate could be used as a reproducible measure of flocculation effectiveness, they developed a relationship between flocculant concentration and refiltration rate, on the basis that the flocculation mechanism consisted of adsorption of polymeric segments of the flocculant onto solid particle sites followed by "bridging" between primary particles. "Bridging" could occur between two primary particles via a common adsorbed multi-segmented polymeric flocculant molecule, or by crossling-ing or hydrogen bonding between adsorbed flocculant molecules. Essentially the derivation led to the Smellie-La Mer eighth-power law

$$\frac{P_o^{1/2}}{(Q-Q')^{1/3}} = A' + B'P_o$$

where P_o is the amount of flocculant added. Q is the

corresponding refiltration rate, Q' is the refiltration rate corresponding to $P_o = 0$. A' and B' are constants such that $(A'/B') = P_m$, is the amount of added flocculant corresponding to the maximum refiltration rate of a series of flocculation systems indexed by the amount of added flocculant. This "eighth power law", however, lacks sensitivity due to its use of the one-eighth power.

3. Silica suspensions and electrokinetic behavior

In 1963 Kane, La Mer and Linford showed that the Smellie-La Mer "eighth-power law" fitted data obtained for flocculation of aqueous silica suspensions using a number of polymeric flocculants (29). Silica was chosen in preference to other solids such as Fuller's earth, kaolinite or montrorillonite, since ion exchange was least evident in the silica suspensions (30). Aware that pH controls adsorption of ionic substances onto the silica surface (31) they attempted to maintain pH at a value of 6.0. The pH level usually found in commercial water purity standards is 5.0 to 6.8 (32).

In 1961 Healy had reported that the electrokinetic behavior of quartz (silica) suspensions with a polyacrylamide flocculant showed correspondence to flocculant adsorption and to flocculation system subsidence behavior (33). In 1966 Dixon, La Mer, Linford et al published results of further work using electrokinetics (34). They investigated

the flocculation behavior of aqueous silica suspensions with a cationic polyelectrolytic polymer as flocculant. The amount of flocculant added which resulted in a zero value of measured electrophoretic mobility corresponded approximately to the optimum measured rate of refiltration for a series of flocculation systems indexed by amount of added flocculant.

Recent results from the same laboratory show that streaming potential measurements, taken by forcing clear electrolytic filtrate to flow through a porous plug of the filtered flocculated solids at a known forcing pressure difference, exhibit a zero value of the Zeta potential calculated from the streaming potential data near the amount of added flocculant required for the optimum rate of refiltration. Although both alternate electrokinetic measurements show similar results near the optimum refiltration rate, the values of Zeta potential calculated from electrophoretic mobility data were in general higher in magnitude than the values calculated from the streaming potential data recorded. This discrepancy was at that time accounted for by the effect of settling of particles on microelectrophoresis measurements. Human error in microscopic tracking was also considered. The electrophoretic mobility data were then thought to lead to unrepresentative calculated Zeta potentials. It was assumed by the investigators that the electrolytic conductivity of the liquid phase used in the streaming potential measurements was high enough to allow the bulk value of specific conducti-

vity, λ, to approximate its value, λ_c, in the small tortuous capillaries of the porous filter bed of flocculated solids. 10^{-3} NaCl had been employed as the streaming medium (35). Their conductivity assumption was probably invalid, due to the size of the "effective" capillaries in the filter beds. The large surface area provided by this small capillary size increases the magnitude of excess electrolytic conduction in the double layer region, relative to conduction in the bulk of the liquid phase. That is, the surface conduction effect was indeed active in these studies.

4. Mechanism

The respective roles of chemical bonding and physical electrostatic repulsion in the mechanism of flocculation were aired in a discussion section following the 1963 paper of Kane, La Mer and Linford (36). The fact, that cationic and anionic flocculants may be used to flocculate negatively charged silica particles from aqueous suspensions (37) seems to support the action of chemical bonding in the mechanism, i.e. chemisorption of the flocculant onto the silica surface followed by bridging between polymeric molecules. However, electrokinetic behavior certainly indicates action of electrostatic forces. Reduction of these physical repulsive forces between solid particles tends to increase collision frequency as discussed in the introduction. Coagulation and flocculation, i.e. suspension instability together

with associated chemical action, are favored by increased collision frequency.

Recent studies (38) show that temperature and silica concentration are important factors in flocculation. Obviously collision frequency is a function of temperature since increased thermal kinetic motion increases collision probability. Silica concentration is a problem in electrophoretic mobility measurements. Dilutions are required to make such measurements in the usual microelectrophoresis equipment. This will be discussed again later. Agitation rate is also known to play a role in flocculation. Large agitation rates tend to break up "flocs" as they are formed, thereby decreasing the average floc size (39). This once more points to the role of physical forces in the overall flocculation mechanism i.e. to physical adsorption and/or hydrogen bonding.

B. Process control of flocculation

1. Electrophoretic mobility and the Zeta-Meter.

The literature has a number of references to use of Zeta potential as a control variable in water clarification processes which use electrolytic coagulants and flocculants. The reported means of calculating the Zeta potential is from microelectrophoretic mobility measurements. Solid charged particles suspended in a liquid medium of known viscosity and dielectric constant are microscopically tracked under the influence of a known D.C. electric field intensity (40-41).

The tracking is performed by observing particles in a suitable microelectrophoresis cell at a plane of focus where the net flow of the suspending electrolyte due to electro-osmosis along the cell wall is zero. It has been shown that when the particle size distribution is wide, larger particles settle out of this plane of focus, thereby erroneously biasing mobility measurements (42). Particles from the larger size end of the distribution, as separated by sedimentation, have been shown to give different mobility measurements than those from the smaller size end of the distribution (43).

In some cases particles of a given sample moved in opposite directions (44). It is known that the electrophoretic mobility varies with the surface charge density (45). Some particles may have different effective charge densities than others due to nonuniform distribution of flocculant adsorption. In fact primary solid particles may vary in surface charge density. Slow addition of flocculant to a suspension was found to better approach the condition of uniform adsorption.

Dilution of a given suspension is required before electrophoretic mobility measurements can be made, when the solid concentration is too high (46). It has been shown that dilution affects flocculation behavior in that it changes the concentration of solids. This change shows itself in particle size distribution determinations (47).

Human bias involved in microscopically tracking solid particles of a polydisperse suspension (one with a wide

distribution of particle size) is only natureal. Much of the poor reproducibility encountered from one technician to another when making the electrophoretic mobility measurements is due to this fact alone.

Regardless of the above difficulties with electrophoretic mobility determinations, a device called the Zeta-Meter (48) is commercially available for EM measurement. Its use in industrial water clarification control is often reported (49-50). For a single technician Zeta-Meter results are precise and work well as a means of process control, as long as dilution procedures are not required. The major points are then the poor reproducibility of EM results from one investigator to another and the nonrepresentative electrokinetic data often obtained by EM studies.

2. Streaming potential measurements and surface conduction.

The disadvantages encountered in using data from electrophoretic mobility measurements to calculate Zeta potentials have led investigators in this laboratory (51) to consider data from streaming potential measurements as an alternate. The streaming potential is the potential difference developed across a filter bed of flocculated solids, when filtrate is forced to flow through the bed at a known forcing pressure difference. Knowledge of the viscosity, dielectric constant and specific conductivity of the filtrate, as it exists in the interstices of the filter bed, allows calculation of Zeta potential. Wide particle size distribution,

human bias and dilution effects are absent. This value of Zeta potential should therefore be representative of the system under study. Precision as well as reproducibility from one technician to another should be greatly improved.

The use of bulk values for the viscosity and dielectric constant usually introduce relatively minor error (52-53). However, for a very dilute electrolytic liquid phase, the specific conductivity, λ_c, exceeds the bulk specific conductivity, λ, of the liquid phase (as measured in a conductivity cell and bridge apparatus) by a noticable amount. The presence of excess ions and dipolar molecules in the double layer (the charge discontinuity occuring at or near the solid - liquid interface) causes additional conduction in the interfacial region (54). This excess conductivity has come to be called the "surface conduction".

One means of accounting for the surface conduction effect was presented by Briggs (55). He measured the resistance of the streaming potential cell along with the usual streaming potential and forcing pressure determination. After streaming measurements Briggs purged the porous plug of his streaming potential cell with an electrolyte, say 0.1 N KCl, whose bulk specific conductivity was large enough to overshadow the surface conduction effect. The corresponding streaming potential cell resistance was again measured and a cell constant calculated. The ratio of this cell constant to the original streaming electrical resistance measurement allowed Briggs to calculate the actual liquid phase specific

conductivity λ_c.

Application of Briggs' method to the electrokinetic study of flocculation systems is not simple. Briggs dealt with plugs of cellulose and similar fibers. If one purges a floc filter bed with say 0.1 N KCl one may remove some of the flocculant from the system. The purged floc bed has then been changed. Even if one were to use a purge liquid containing polymer, the chances of changing the floc bed are unknown.

It is being proposed that Briggs' treatment can be achieved as follows. A given series of flocculation systems is studied over a series of KCl concentrations. It is assumed, for example, that the flocculation system for 10^{-2} N KCl is not far different from that for 10^{-4} N KCl with respect to the flocculation mechanism and resulting floc bed. An apparent cell constant (calculated from the bulk liquid specific conductivity λ) at the 10^{-2} N KCl level might then be applied as the actual cell constant (as would be calculated from the effective specific conductivity λ_c) at lower KCl levels, where the apparent cell constant is in error due to surface conduction. It would be assumed that $\lambda = \lambda_c$ at 10^{-2} N KCl for such an example.

When dealing with a single capillary, values of the empirical parameter called "specific surface conductivity", χ, have been reported (56). The exact dimensions of the capillary must be known, and the assumption must be made that the bulk conduction and the surface conduction can be

represented as parallel electrical resistors. The calculation of the dimension of the "effective" capillaries in a porous plug is not easy, especially when the plug is made up of particles whose size distributions is wide, e.g. a floc filter bed. Any attempt to compare results reported in the literature meet with extreme difficulty, except with respect to order of magnitude (57-59). Use of a consistant set of bed parameters, namely porosity and surface - volume mean diamter (60) might lead to better precision in such comparisons.

In 1959, Zucker attempted to rigorously account for the surface conduction effect in porous plug streaming potential cells. He started the derivation of the equation, used to calculate Zeta potential from streaming potential data, from the concepts of moments of electrical charge and of the Onsager conductivity relation (61). His derived equation is applicable to monodisperse, i.e. single size and shape, particle beds. Otherwise, statistical estimated of particle size must be used, thereby adding uncertainty to results calculated from his equation. However, it is noted that essentially Zucker calculated a cell constant "a priori" from the bed parameters and used both streaming potential and resistance measurements. Hence his method is similar to Briggs' idea (62).

Another possible way to cope with the surface conduction effect has been reported by Oulman and Baumann (63). They employ an extrapolation of calculated apparent Zeta potentials,

i.e. those calculated using bulk specific conductivities, for a set of bulk electrolyte concentrations. They also report values of the "specific surface conductivity" based on a calculation similar to the relations of the single capillary. They use some mean particle size but omit the use of bed porosity, therefore making the reported values of specific surface conductivity really only qualitative. Theoretical variation of "specific surface conductivity" with bulk electrolyte concentration as noted by Overbeek (64) shows that the technique of Culman and Baumann may be invalid. They give an equation of the form

$$\frac{1}{\zeta} = \frac{1}{\zeta_T} + \frac{4\chi}{\zeta_T d} \cdot \frac{1}{\lambda}$$

where ζ is the apparent Zeta potential, ζ_T is their actual Zeta potential, χ is the specific surface conductivity, d is their mean particle diameter, and λ is the bulk liquid phase specific conductivity. They plot $\frac{1}{\zeta}$ against $\frac{1}{\lambda}$ and note that the slope is $\frac{4\chi}{\zeta_T d}$. They apparently assume that the straight line relation is valid for all values of λ so that the slope $\frac{4\chi}{\zeta_T d}$ is a constant. But ζ_T varies with λ (65) as does χ (66).

In fact it is entirely possible that with increasing λ, χ increases while ζ_T decreases due to diffuse double layer compression, thereby increasing the slope $\frac{4\chi}{\zeta_T d}$. The Culman and Baumann data even give indications of this effect (67).

Since the "specific surface conductivity" χ theoretically is a function of double layer ion mobilities (68) then it should depict variation in the double layer constituancy. χ values reported in the literature (69-73) have been said to reflect suspension stability in the same sense as Zeta potential i.e. subject to experimental verification (74).

A third possibility to account for the surface conduction effect is to measure the streaming current directly as a function of the pressure difference. This replaces measurement of both streaming potential and cell resistance. Care must be taken that the ammeter circuit employed has effectively zero resistance (75). Care must be taken that the streaming potential cell electrodes are non-polarizable, i.e. reversible, both at the streaming current magnitudes measured and with respect to the flocculation system being studied (76). Organic adsorbates, i.e. like cationic polyelectrolytic polymeric flocculant used in the studies reported, may have an effect on the reversibilities of the Ag, AgCl electrodes (77-78). It is therefore highly advisable to employ the usual streaming potential measurements, that is, measurement of the streaming potential using a high impedance, e.g. 10^{14} ohm, voltmeter, so that the current flowing across the electrode - liquid phase interface is negligibly small, thereby suppressing electrode polarization; and measurement of the streaming cell resistance using a high frequency AC Wheatstone bridge thereby further suppressing electrode polarization.

C. Silicates

One reason that the aqueous silica system is often chosen for electrokinetic studies is its ease of fabrication. For example consider the measurement of streaming potentials for electrolytes forced through glass capillaries. Or consider the suspension of powdered silica in liquid electrolyte, as in the work presented here.

Freshly cleaved crystalline silica (quartz) has an amorphous surface layer. The surface of solid amorphous silica has been shown to have an inherent negative charge when fully charged with hydroxyl ions (i.e. at low values of liquid phase pH.). At pH 6 the silica surface would then be expected to have a net negative charge (79).

Polar groups of organic molecules adsorb strongly onto a silicate surface. The presence of more than one polar group per molecule further enhances adsorption, as does presence of a large number of non-polar hydrocarbon groups (80). A polyethyleneimine, i.e. $CH_2\underset{NH}{\diagup}CH\text{-}(CH_2CHNH)_n NH_2$ would therefore probably adsorb well onto the silicate surface.

Some alkali metal ions, viz. Na^+, specifically adsorb onto the silicate surface and thereby inhibit adsorption of other molecules (81). Hence KCl has been chosen in place of NaCl as the general liquid phase electrolyte of the flocculation systems in the present work.

D. Polyethyleneimines

Polyethyleneimines (PEI's) are high molecular weight polymers of the monomer $CH_2=CHNH_2$ with the general structure

$$CH_2\text{-}CH(CH_2CHNH)_n NH_2$$
$$\backslash\ 2\ /$$
$$NH$$

where n varies from 25 to 770. The degree of crosslinking depends on preparation methods. Appreciable branching of the base chain is evident according to studies reported by Dixon et al (82). It would appear that the molecules of PEI satisfy the conditions for good adsorption onto the amorphous silicate surface layer of powerdered silica as described earlier.

III. Theory

A. Electrokinetics

The first of the electrokinetic phenomena was noted by Reuse in 1809. Liquid electrolyte was observed to move through a solid porous diaphram upon application of an electric field across the diaphram. The effect was termed electro-osmosis. Similarly when an electric field was impressed across a tube containing a dilute suspension of solid in an electrolytic medium, the solids moved with respect to the liquid phase. This came to be called electrophoresis. In 1859 Quinke noticed that if a liquid electrolyte was forced to flow through a capillary or porous diaphram, an emf was generated between any two points along the line of flow. Similarly, in 1880 Dorn reported that an emf was generated between any two points in the direction of settling when solid particles were allowed to settle through a liquid electrolyte. This was called the sedimentation potential or Dorn effect (83).

The term electrokinetics implies the movement of one phase with respect to a second phase upon application of an electric field which can act along the phase boundary. The inverse case, i.e. the generation of an emf along the phase boundary upon forcing one phase to move with respect to the other, is also then classed as being electrokinetic.

B. Double Layer

When a two phase system consists of a liquid phase electrolyte and a solid phase, a charge discontinuity occurs at the phase boundary. The effective solid surface is not electrically neutral but maintains a net charge dependent upon the physical and chemical nature of the system. This surface simultaneously attracts oppositely charged ions and dipolar molecules from the bulk of the liquid electrolyte to achieve electrical neutrality for the entire two phase system. Combination of the net charge of the effective solid surface with the attracted liquid phase ions and dipolar molecules make up what is called the "double layer" (84).

The first model of the double layer was developed by Helmholtz in 1879. He pictured two oppositely charged layers separated by a fixed distance. The double layer was represented by an electrical condenser of constant capacity whose parallel plates are of the order of one molecular diameter apart (85). The capacity of a condenser is by definition the net charge on one of the plates per unit potential drop across the plates. In 1904 Perrin applied the laws of electrostatics to this condenser to try to calculate the potential difference ϕ across the double layer.

$$\phi = \frac{4\pi\sigma_o \delta'}{D} \qquad [1]$$

where σ_o is the surface charge density of one plate, δ' is the distance between the plates and D is the dielectric

constant of the liquid between the plates (86).

Realizing the existence of normal thermal kinetic motion in the bulk liquid phase and the effect of the charged solid surface on the normal distribution of particles in the liquid phase, Gouy in 1910 and Chapman in 1913 independently arrived at a model to account for this. They considered the liquid phase side of the double layer to be diffuse in nature, containing both ions which are charged oppositely to the effective solid surface as well as ions of the same charge as the effective solid surface. Boltzmann concentration distributions were assumed for these liquid phase ions and the capacity of this model was calculated. However the calculated capacities did not agree with experimentally observed values (87).

In 1924 Stern suggested that a new model be used, incorporating both the model of Helmholtz and that of Gouy and Chapman. Stern noticed the variance of the measured double layer capacity with experimental conditions. Also he noted the influence of electrolytes on the value of the potential difference ζ between the "plane of shear", formed during electrokinetic measurements, and the bulk of the liquid phase. The "shear plane" is actually not a plane but a region separating two other regions, one of which is in motion relative to the other. This "shear plane" does not necessarily start at the solid-liquid interface, but at a distance of one or two atomic diameters out into the liquid phase, especially when there is specific adsorption. The solid surface is often

jagged and therefore the distance between the "shear plane" and the solid-liquid interface is not easily defined. This is one reason that an accepteable physical meaning for Zeta potential, ζ, is still in question. Stern divided the liquid phase side of the double layer into two parts, an inner layer of strongly adsorbed ions immediately next to the solid phase and an outer diffuse layer of ions extending into the liquid phase. The inner adsorbed layer was to have the dimension of about one molecular diameter and the outer diffuse layer was to follow the Boltzmann concentration distribution. Stern had thus accounted for the size of ions, with regard to their plane of closest possible approach to the solid surface. Gouy and Chapman had omitted any consideration of ionic size, thereby following an assumption later to be taken by Debye and Hückel in the theory of the ion atmosphere. Stern argued that the potential difference ζ between the "plane of shear" and the bulk of the liquid phase was the value measured by electrokinetic studies. The thermodynamically reversible Galvani potential difference ϕ occuring between the bulk solid phase and the bulk liquid phase remains constant according to Stern's model. This agrees with experiment (88). With ϕ as the Galvani potential difference, ψ_1 as the potential difference between the bulk liquid phase and the plane, which separates the inner adsorbed layer and outer diffuse layer, and ζ as the potential difference measured during electrokinetic studies, Figure 1 is drawn.

Figure 1

$\bar{\psi}$ - y diagram

$\bar{\psi}$	potential with respect to the bulk liquid phase as a function of y
y	distance from the solid - liquid interface
y_s	distance of the electrokinetic shear plane from the solid-liquid interface
ζ	Zeta potential, the potential difference between the bulk liquid phase and the electrokinetic "shear plane"
ψ_1	potential difference between the bulk liquid phase and the plane separating the inner adsorbed Stern layer from the outer diffuse Stern layer
ϕ	Galvani potential, the potential difference between the bulk liquid phase and the bulk solid phase

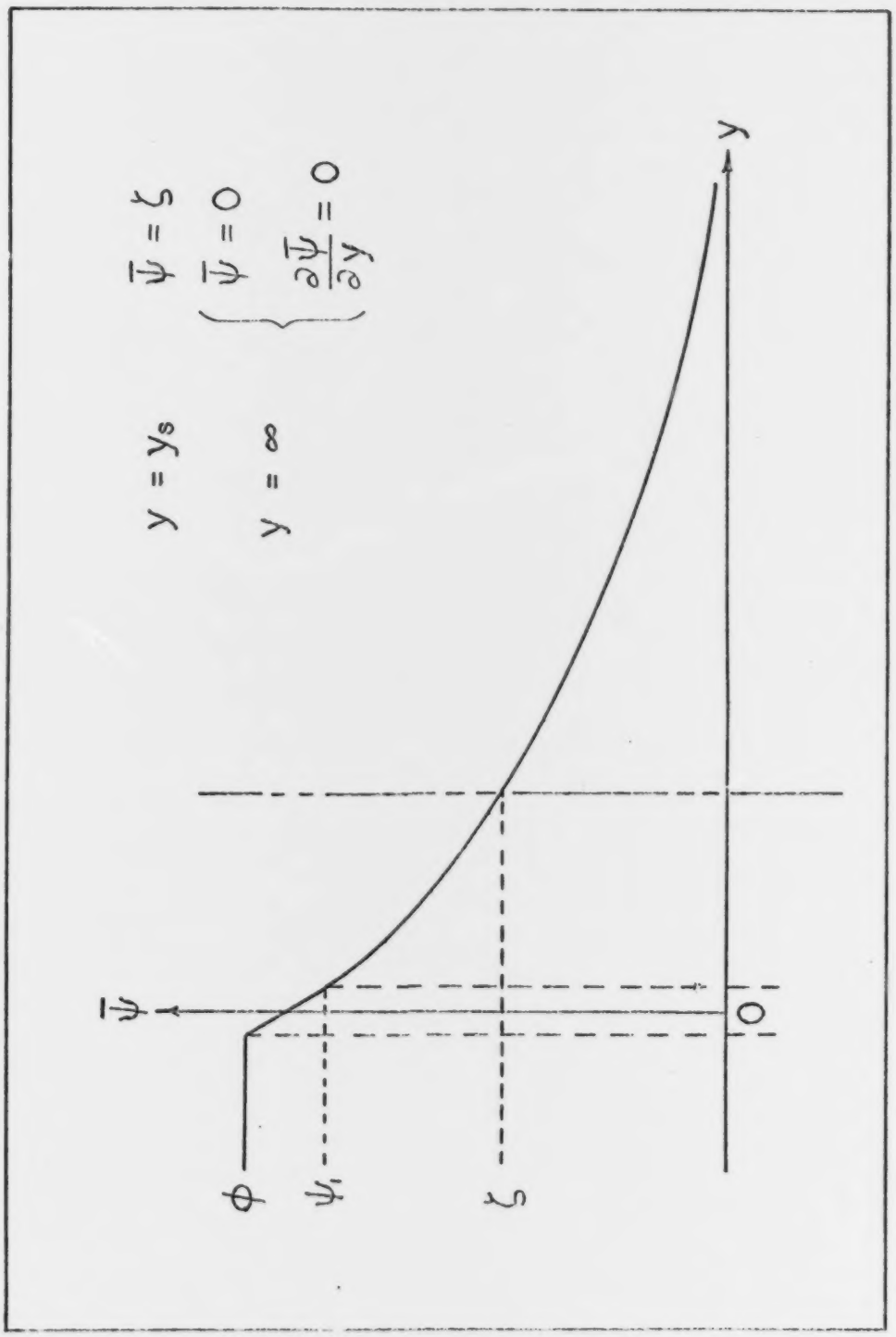
y
$\bar{\psi} = \zeta$
$\bar{\psi} = 0$
$\frac{\partial \bar{\psi}}{\partial y} = 0$
$y = y_s$
$y = \infty$
$\bar{\psi}$
0
ϕ
ψ_i
ζ

In 1947 Grahame (89) proposed modeling Stern's inner adsorbed layer as two parts to account for the difference in dimension between adsorbed anions and adsorbed cations. However, this much attention to detail does not overshadow the original Stern model.

Equation [1] can also be arrived at from the Gouy-Chapman model when the liquid electrolyte content is sufficiently low (90). An equation of the same form can then be applied to the electrokinetically mobile liquid phase part of the double layer. That is, the Zeta potential ζ can be calculated as

$$\zeta = \frac{4\pi\sigma\delta}{D} \qquad [2]$$

where δ is the "effective" distance between the "plane of shear" and the point of zero net charge density in the bulk liquid phase. "Effective" distance, referring to the diffuse character of the liquid side of the double layer, is the distance between plates of a corresponding "effective" capacitor. $-\sigma$ is the net effective surface charge density on the bulk liquid phase side of the "Shear plane". Surface charge density refers to charge density based on surface area rather than on volume. This is what is generally done for volumetric configurations where one dimension is extremely small. D is now the effective dielectric constant of the liquid in the mobile part of the double layer.

C. Electrokinetics and Zeta potential

1. Electrophoretic mobility

During electro-osmosis, the electrical force causing

motion of the liquid phase with respect to the solid phase is balanced at steady state by the frictional force which opposes this motion. The electrical force is $\xi\sigma$ where ξ is the applied electric field (potential gradient), and $-\sigma$ is the surface charge density on the mobile liquid side of the "shear plane". The friction force is $\eta\bar{u}/\delta$ where η is the liquid viscosity, δ is the effective thickness of the part of the double layer in motion with respect to the solid phase and $\bar{u}$ is the uniform linear velocity attained by the bulk liquid phase. Equating opposing forces at steady state

$$\eta\bar{u}/\delta = \xi\sigma \qquad [3]$$

Substituting for δ from equation [2] and rearranging, then

$$\zeta = (4\pi\eta\bar{u})/(D\xi) \qquad [4]$$

Since in electrophoresis the relative motion is just reversed then it is equally valid to write

$$\zeta = \frac{4\pi\eta}{D} U_e \qquad [5]$$

where U_e is defined as the electrophoretic mobility, $\bar{u}/\xi$ (91).

From equation [3]

$$U_e = \frac{\bar{u}}{\xi} = \frac{\sigma\delta}{\eta} \qquad [6]$$

i.e. the electrophoretic mobility depends on the net effective surface charge density σ. It is possible that σ may vary from one particle to another in a flocculation system,

depending on locations of adsorption sites on the solid particles and depending on the chemical structure of the adsorbed flocculant. Therefore wide scatter of U_e might be expected in a given system. Variation of measured U_e with particle size was reported from this laboratory (92) for such flocculation systems.

2. Streaming potential

An equation relating the measurable parameters of the streaming potential effect with the Zeta potential, ζ, is often derived as follows (93-94). Assuming laminar flow, the Poiseuille equation for the flow of a viscous liquid through a cylindrical capillary tube shows that

$$u = \Delta P(r^2 - x^2)/(4\eta L) \qquad [7]$$

where ΔP is the pressure difference between two points spaced L distance apart in the tube. The tube has radius r and the liquid flowing in the tube has viscosity η. "x" is the distance from the center of the tube to a point where the linear velocity is u (see Figure 2).

For a charged solid-liquid electrolyte system there exists a charge discontinuity at the solid-liquid interface, i.e. an electrical double layer as described earlier. During motion between the solid and liquid phases, there exists a "plane of shear" in the liquid phase close to the solid-liquid interface The distance between the interface and the shear plane is of the order of magnitude of several atomic diameters. The liquid which lies between this "shear plane" and the solid surface

Figure 2

Streaming Potential Capillary

L	length of capillary
r	radius of capillary
x	distance from center of capillary
u	linear velocity at distance x
s	distance of electrokinetic shear plane from center of capillary

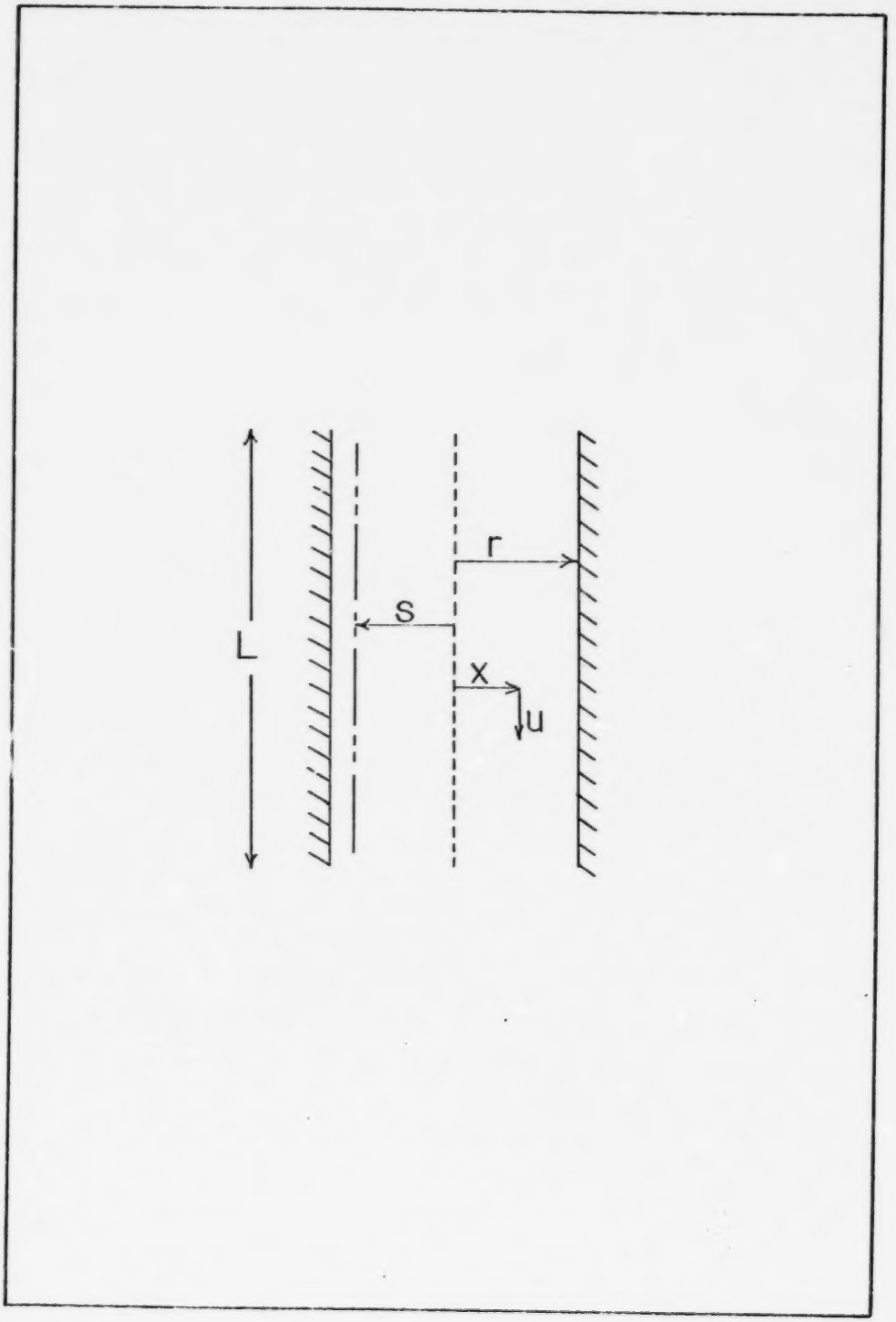
L
s
r
x
u

remains fixed to the solid surface. Using the Stern model of the double layer, the charge imbalance continues for many atomic diameters beyond the "shear plane". Therefore any movement of this portion of the double layer would result in a charge transport which in effect is the streaming current I_s. It is calculated for the described cylindrical capillary as:

$$I_s = \int_o^s 2\pi x \rho u dx \qquad [8]$$

where ρ is the volumetric charge density, and s is the distance of the shear plane from the center of the capillary. With infinite external resistance the relative motion of the charged particles will develop a potential gradient through the cell and when the steady state condition is reached no further net current flows. If a zero resistance ammeter is placed across the terminals of the streaming potential cell the current flowing will equal I_s at steady state if no polarization occurs at the electrodes. This current, I_s, would equal the value of the streaming potential divided by the electrolytic resistance of the cell. If R_c is the resistance of and C_c the conductance of the total liquid in the capillary then from the relations of electrolytic conduction measurement,

$$C_c = 1/R_c = \lambda_c \pi r^2/L \qquad [9]$$

thereby defining λ_c as the effective specific electrolytic conductivity of the total liquid in the tube. By Ohm's law

the streaming potential E_s may be defined as

$$E_s = I_s R_c = I_s L/(\pi r^2 \lambda_c) \qquad [10]$$

Upon combining of equations [8] and [10],

$$E_s = [-L/(\pi r^2 \lambda_c)] \int_o^s 2\pi x \rho u dx \qquad [11]$$

Now Poisson's relation between the volumetric charge density ρ and the electrical potential $\bar{\psi}$ in cylindrical coordinates is

$$(1/x)[d/dx(x d\bar{\psi}/dx)] = -4\pi\rho/D \qquad [12]$$

where D is the dielectric constant. Substituting for ρ from equation [12] and u from equation [7] into equation [11], and evaluating the resulting integral, assuming that the effective thickness, δ, of the mobile liquid part of the double layer is much less than the capillary radius, r, and that the "shear plane" is close to the capillary wall, then

$$\zeta = (4\pi\eta\lambda_c/D)(E_s/\Delta P) \qquad [13]$$

Equation [13] is the equation for calculating the Zeta potential, ζ, from streaming potential data. η, D and λ_c must be values for the liquid as it exists in the capillary. Equation [13] is independent of the capillary dimensions. Provided all derivation assumptions are met, measurement of E_s and ΔP along with η, D and λ_c complete the experimental evaluation of ζ. The ratio $E_s/\Delta P$ should be constant for a given set of experimental conditions and a given system.

a. Electrolytic conductance measurement

If a cubic centimeter of a liquid electrolyte acts as a conductor (see Figure 3), and if a potential difference E is impressed across this conductor from face abcd to face efgh such that current will flow as indicated by I and the arrow, then this current, I, is experimentally directly proportional to E and to the cross-sectional area A of face abcd or efgh, and inversely proportional to the length L' across which E is impressed. That is

$$I \propto EA/L' \qquad [14]$$

We can then define the constant λ such that

$$I = \lambda EA/L' \qquad [15]$$

By Ohm's law $E = IR$ where R is the electrical resistance of liquid in the volume considered, so that

$$C = 1/R = \lambda/(L'/A) \qquad [16]$$

where C is defined as the "conductance" of the liquid electrolyte in the volume considered. λ is called the specific conductivity of the electrolytic liquid and is an intensive property. That is, the "specific conductivity", λ, with dimensions of $ohm^{-1}cm^{-1}$ or more simply mho/cm, is the "conductance" of a "unit cube" of the electrolyte.

In the design of conductivity cell the term (L'/A) is called the cell constant, K, since it depends on the configuration of the cell. Ideally, L' is the distance between the electrodes of the cell used to impress the voltage E, and A is the cross-sectional area of each of the electrodes perpendicular to the direction of current flow. However, in

Figure 3

Conductivity Cube

I	current
L'	length in direction of current flow I
abcd	face of area A which is perpendicular to current flow I
efgh	face of area A which is perpendicular to current flow I

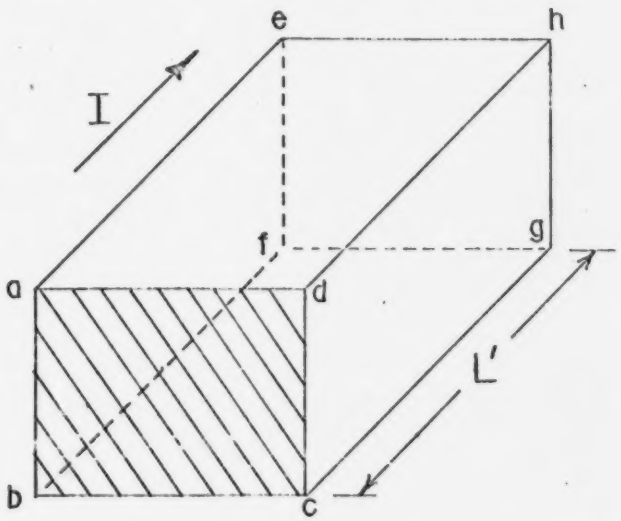
e
h
I
f
g
a
d
L'
b
c

practice, due to the current distribution being dependent on actual cell design, the cell constant, K, must be measured for each cell by noting the cell resistance when it is filled with an electrolyte of known specific conductivity. Noting that the dimension of $K = L'/A$ is cm^{-1}, then

$$C = \lambda/K \qquad [17]$$

b. Surface conduction

In the derivation of equation [13] it was assumed that the effective dimension of the mobile part of the double layer was much smaller than the radius of the capillary under consideration. In the systems being studied in the present work this assumption is usually valid, as long as the bulk electrolyte concentration of the liquid phase is sufficiently high, say $\geq 10^{-4}$ N.

Application of equation [13] also assumes that the values of η, D, and λ_c are known or can be adequately estimated. The use of bulk liquid phase values for η and D have been shown in the literature to introduce only minor error in most instances (95-96). Therefore most reported values of the calculated Zeta potential, ζ, assume bulk values for η and D. When the "effective" capillary radius is extremely small as in the case of a packed bed of minute solid particles and/or when the electrolyte content of the liquid phase is very low then λ_c cannot be approximated by its bulk liquid phase value, λ. The behavior of the excess charges present in the double layer in the form of ions and dipolar molecules must be considered.

The presence of these excess charges increases the total effective value of electrolytic conductance, C_c, in a typical capillary so that C_c is greater than the conductance C of a similarly configurated volume of liquid electrolyte in the absence of the double layer. Since the cause of the excess conductance occurs in the double layer region at and near the solid-liquid phase boundary, its value is called surface conductance, C_s. Considering the excess surface conduction as occuring in a path parallel to the bulk liquid conduction path, Figure 4 is drawn, where R_s is the reciprocal of the surface conductance, C_s, and R is the reciprocal of the bulk conductance, C. That is

$$C_c = C + C_s \qquad [18]$$

where C_c is the total "conductance" of the liquid electrolyte as it exists in the capillary. If the actual cell constant, K, of the capillary (with electrodes placed at either end to form a conductivity cell) can be determined then one might write

$$C = \lambda/K \qquad [19]$$

and

$$1/R_c = C_c = \lambda_c/K \qquad [20]$$

where λ is the bulk value of the liquid phase specific conductivity measured outside the capillary in an ordinary conductivity cell, where λ_c is the value of the specific conductivity for the liquid as it exists in the capillary, and where R_c is the measurable resitance of the liquid filled

Figure 4

Alternate Conduction Paths

R	resistance which is the reciprocal of the bulk conductance C
R_s	resistance which is the reciprocal of the surface conductance C_s

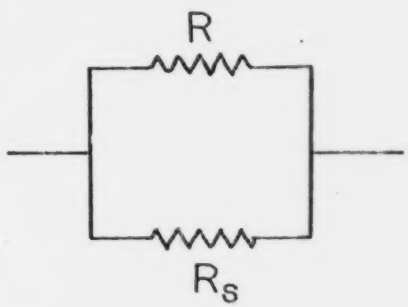
R
R_s

capillary. Equation [20] is the basis for Briggs' method of accounting for surface conduction when calculating from streaming potential data (97). Essentially Briggs determined the cell constant, K, after purging the capillary (or in his studies a packed bed of tortuous effective capillaries) with an electrolyte whose bulk specific conductivity, λ, is high enough to be an adequate estimate of the capillary effective specific conductivity, λ_c.

Combining equations [18], [19], and [20]

$$(\lambda_c/K) = (\lambda/K) + C_s \qquad [21]$$

If one considers the annular volume of the streaming capillary which is that particular volume occupied by the mobile part of the electrical double layer and if one applies the relations of electrolytic conductance measurement to this annular volume, then

$$C_s = \lambda_s/K_s \qquad [22]$$

where the cell constant, K_s, applies <u>only</u> to this annular volume. One of the dimensions of this annular volume, namely the effective dimension δ of the mobile part of the double layer, is fixed by the properties of the electrochemical system. The area A_s of the conductivity cell represented by the annulus can therefore be shown to be

$$A_s = 2\pi r\delta \qquad [23]$$

Hence the cell constant, K_s, for the annulus becomes

$$K_s = L/A_s = L/(2\pi r\delta) \qquad [24]$$

Since δ is dependent on the electrochemical system and L and r are dependent on the annular configuration a new constant, M, is defined as

$$M = (L/2\pi r) \qquad [25]$$

and therefore from equations [21], [22], and [25]

$$(\lambda_c/K) = (\lambda/K) + (\lambda_s/M) \qquad [26]$$

Letting $\lambda_s \delta = \chi$ and calling χ the "specific surface conductivity", then χ has units of ($ohm^{-1} cm^{-1} cm$) or simply ohm^{-1}, often written as mho. Now

$$\lambda_c = \lambda + [\chi/(M/K)] \qquad [27]$$

But $K = L/\pi r^2$ for a given cylindrical capillary of radius r and $M = L/2\pi r$. Therefore M/K equals r/2. It is also seen that the hydraulic radius r_H of the cylindrical capillary equals r/2 since

$$r_H = S/\Omega = (\pi r^2)/(2\pi r) = M/K = r/2 \qquad [28]$$

where S is the cross-sectional area perpendicular to flow and Ω is the wetted perimeter perpendicular to flow. Equation [27] resembles equations found in literature (98-102).

For application of equation [27] to a packed bed which is effectively a bundle of tortuous capillaries, the ratio of M/K can be estimated from a measurement of the hydraulic radius, r_H, of a given packed bed (103). Therefore

$$\lambda_c = \lambda + (\chi/r_H) \qquad [29]$$

The value of the hydraulic radius, r_H, can be estimated from a weight basis cumulative percent particle size distribution and the bed porosity ϵ (104). Also

$$r_H = [\epsilon/(1-\epsilon)](v_p/s_p) \qquad [30]$$

where v_p is the mean equivalent particle volume and s_p is the mean equivalent particle surface area. The surface-volume mean particle diameter d_{sv} is defined as

$$d_{sv} = (\Sigma f d^3)/(\Sigma f d^2) \qquad [31]$$

where d is a particle diameter and f the frequency of its occurance in a given size distribution. Kane, La Mer and Linford mention that the primary silica particles, under consideration in the present work, are about spherical in shape (105). The shape of actual flocs is irregular. Assuming <u>equivalent spherical dimensions</u> for a given floc particle, then

$$v_p/s_p = d_{sv}/6 \qquad [32]$$

so that

$$r_H = [\epsilon/(1-\epsilon)][d_{sv}/6] \qquad [33]$$

Considering equations [21], [27], and [28] and letting K_a equal λR_c where R_c is the measured resistance of a streaming potential cell made up of a packed floc bed filled with liquid electrolyte of bulk specific conductivity, λ,

$$K/K_a = [1 + (C_s/C)] = [1 + (1/r_H)(\chi/\lambda)] \qquad [34]$$

Substituting from equation [33] for r_H and solving for χ

$$\chi = [(K/K_a) - 1] [\epsilon/(1-\epsilon)] [d_{sv}/6] [\lambda] \quad [35]$$

Equation [35] allows calculation of values for the specific surface conductivity, χ, in at least a semiquantitative manner depending on the statistical determation of the value of d_{sv}.

Infiltration Specifications

The average infiltration specification was determined by weighted average with respect to miles of sewer and with respect to daily flow. These averages are as follows:

571 gal./in of diam./mile/day weighted according to miles of sewer.
486 gal./in of diam./mile/day weighted according to flow.

75% of those answering had an infiltration spec.

Sewage Flow

Total Flow Sampled .....549 MGD
Treated Flow .....394 MGD
% of Total Being Treated 71.8%

IV. Laboratory experiments

A. Materials and chemicals

The chemicals and materials used in the present work are listed here f . reference:

1. Primary solids: Min-U-Sil, a graded crystalline silica available from Pennsylvania Glass Sand Corp., Pittsburgh, Pa., in nominal sizes of 5, 10, 15 and 30 microns, where the nominal size refers to the fact that 98 wt% of the particles have diameters less than the nominal size.
2. Suspension medium: dilute aqueous solutions of KCl made up from 10^6 ohm-cm conductivity water.
3. Flocculating agent: ET 723, a cationic polyelectrolytic organic polymer which is a polyethyleneimine (PEI) of M.W. 32000, available from Dow Chemical Co., Midland, Michigan.
4. Filter supports: 1.2 micron Millipore supports. MF type RA available from Millipore Filter Corp., Bedford, Mass. The millipore support used is composed of short capillary openings and therefore would contribute to any streaming potential measurements. This has been shown to be negligible since at a given Zeta potential the streaming potential is directly proportional to the pressure drop. In a bed composed of the floc on top of the millipore support there are two pressure drops in series. As an example, when the total pressure drop is of the order of 74 cm

of mercury the manufacturers flow vs. pressure data can be extrapolated to indicate the pressure drop through the filter support to be of the order of 0.01 centimeter of mercury. This negligible pressure drop cannot produce a measurable change in the streaming potential. Therefore, the streaming potential measured can be considered as the streaming potential produced in the floc bed alone.

B. Equipment

Specialized equipment used is listed below.

1. Streaming Potential Cell.

The actual streaming potential cell consisted of a vertical piece of 9 mm bore pyrex tube to which two closely matched Ag,AgCl electrodes (described below) were fitted. The details are shown in Figure 5. Note that the cell could be disassembled just above the bottom electrode to allow a filter support to be clamped between precision ground glass faces. An integral glass frit provided support for the bottom electrode without impeding liquid flow.

2. Ag,AgCl Electrodes

The streaming potential cell electrodes were electrolytically prepared Ag,AgCl electrodes. A piece of silver mesh was cut to fit the bore of the streaming potential cell and then attached with a silver pin to the end of a silver rod (see Figure 6). The assembled

Figure 5

Streaming Potential Cell

A	9 mm pyrex glass tube
B	precision ground glass
C	glass frit
D	filter support
E	Ag,AgCl electrodes

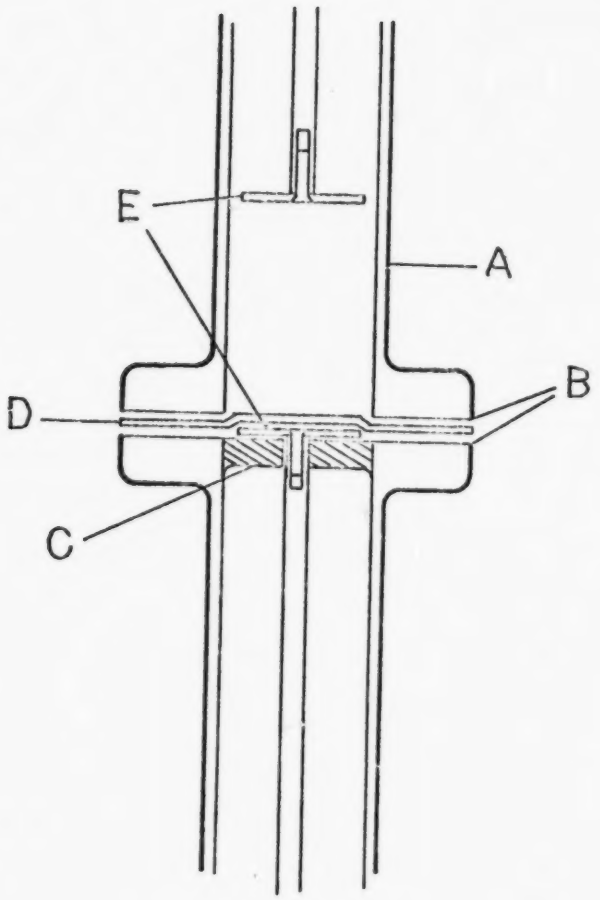
E
A
B
D
C

Figure 6

Ag,AgCl electrode

A silver mesh

B silver pin

C silver rod

D silver chloride coating

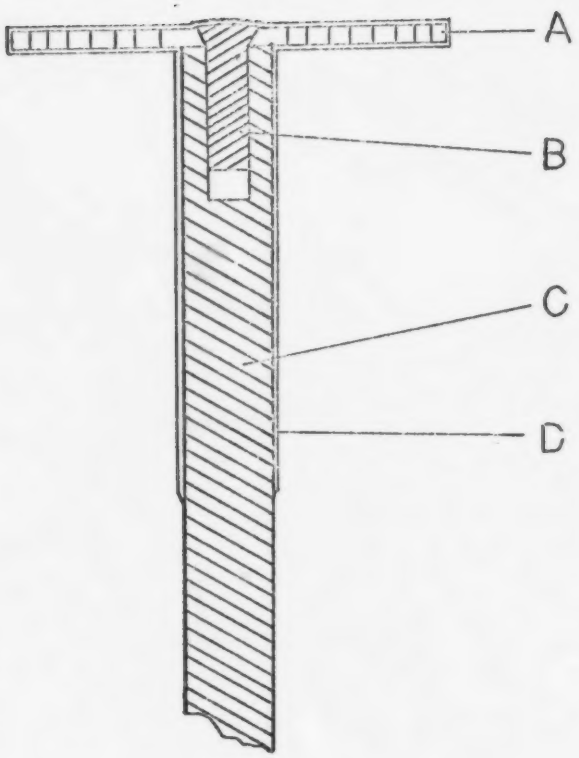
A
B
C
D

electrode was then silver plated in a AgCN bath for three hours at a current density of about 3 ma/cm^2 using a silver sheet as the anode. The Ag plated Ag-electrode was then anodized in 0.1 N HCl with the silver electrode as the anode and the silver sheet as the cathode. Anodizing was carried out for 30 minutes at approximately 3 ma/cm^2 current density. Two electrodes were prepared for each streaming potential cell. The completed electrodes were aged for about one week before use and found to be stable for several months.

3. Streaming Apparatus

The streaming apparatus was based on the design of Martin and Gortner (106) with modification to allow for a vertical streaming potential cell with a movable top electrode (see Figure 7 and 8). A starret micrometer head attached to the top electrode allowed determination of the depth of the floc bed between the two electrodes. The top electrode side's liquid reservoir was open to the atmosphere. The bottom electrode side's liquid reservoir was connected to house vacuum using a Cartesian diver manostat control (Fisher Scientific, New York). Application of vacuum caused liquid to flow through the streaming potential cell. When the entire streaming potential cell was removed (including electrode O-ring seals and micrometer depth gage) it was possible to directly attach a flow-type conductivity cell between the two reservoirs (see Figure 9). This allowed

Figure 7

Assembly of Streaming Potential Cell

A	Starrett micrometer depth gage
B	aluminum flanges
C	rubber gaskets
D	silver rod
E	nylon connector
F	silver, silver chloride electrodes
G	silver pin
H	fritted glass disc
I	filter support
J	deposited bed
K	O-rings

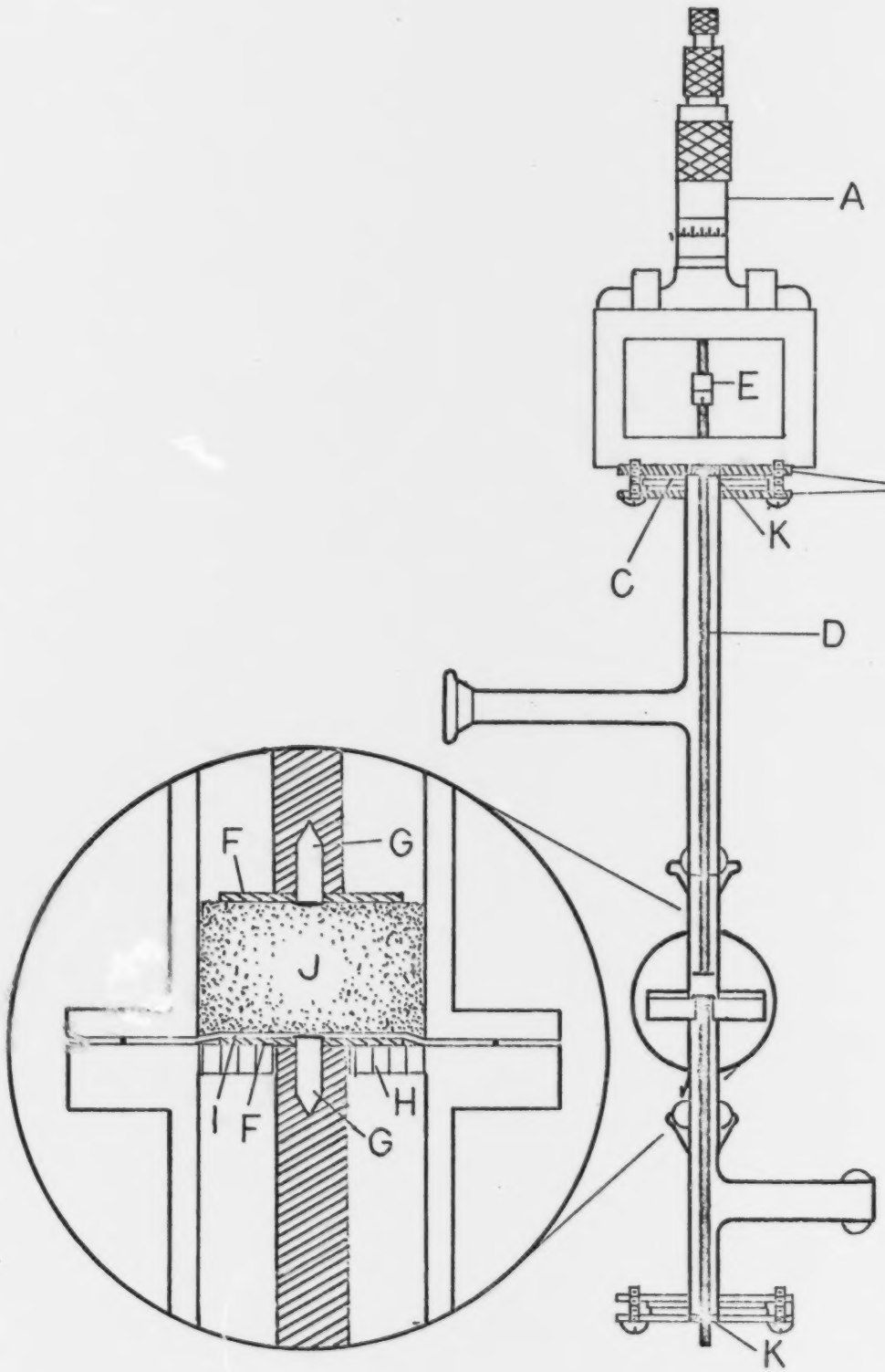
A
E
B
K
C
D
F
G
J
I
F
G
H
K

Figure 8

Streaming Potential Apparatus

A one liter liquid resevoir

B streaming potential cell

C manometer

D surge tank

E vacuum pump

F cartesian manostate to control vacuum

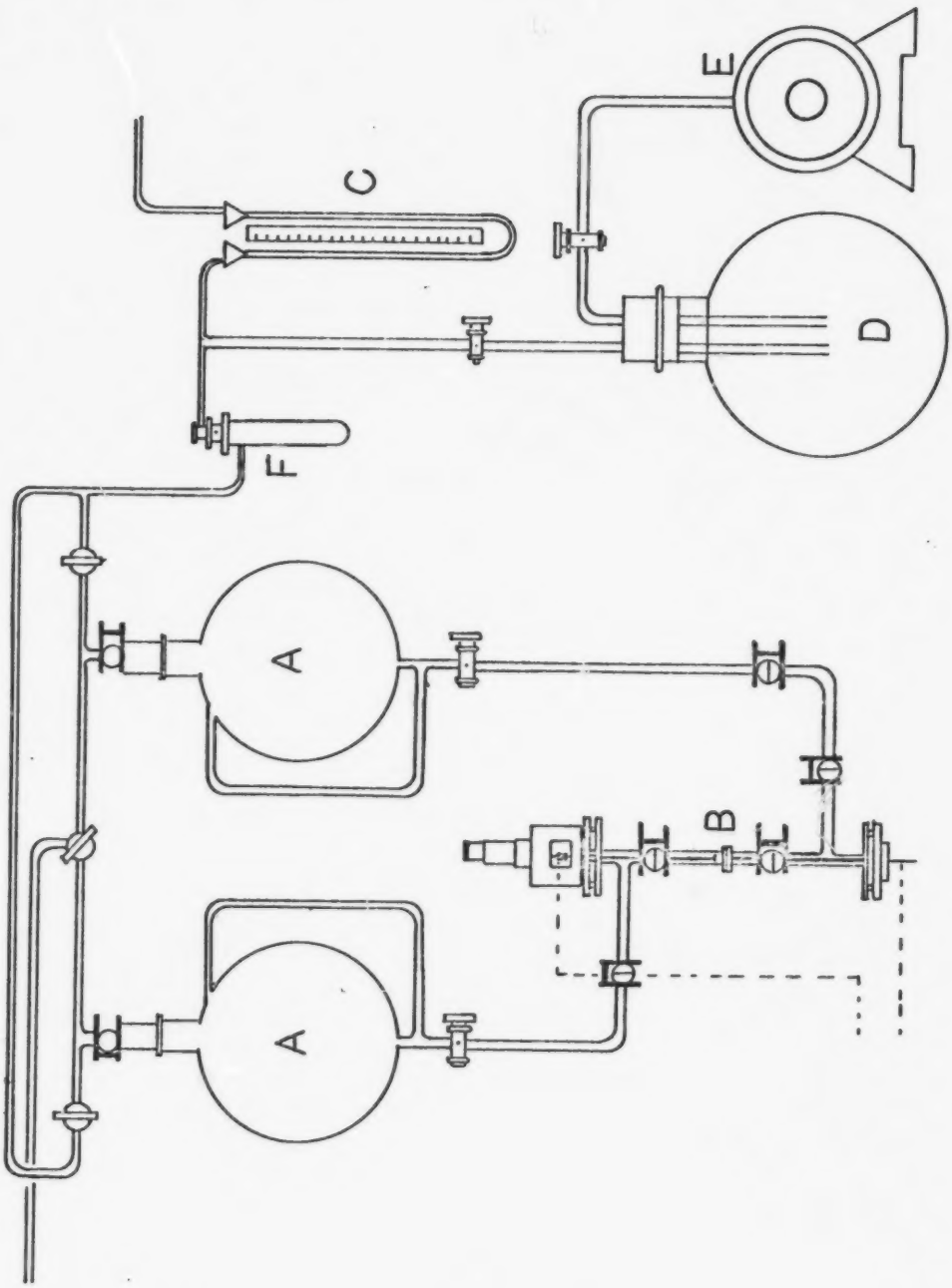
E
C
D
F
A
B
A

Figure 9

Streaming Potential Apparatus
with Conductivity Cell Attached

A Conductivity cell

B Platinized platinum electrodes

C Wheatstone bridge

D Streaming potential apparatus

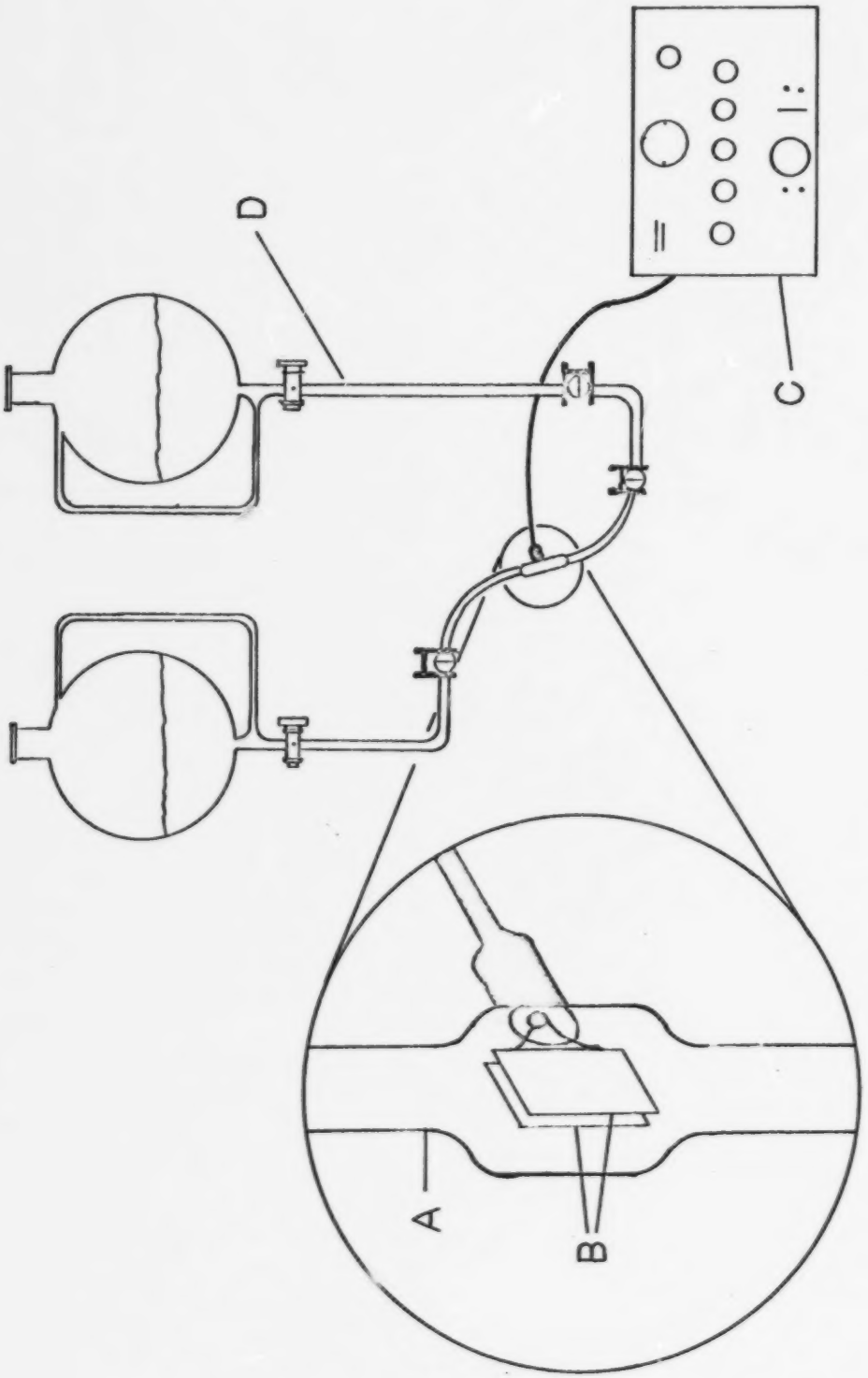
D
C
A
B

accurate measurement of bulk liquid specific conductivity under the same room temperature conditions affecting the actual streaming potential cell.

4. Conductivity Cell

A 0.0100 cm^{-1} cell constant flow-type pyrex conductivity cell (Beckman Instruments, Cedar Grove, N.J.) was used to measure bulk values of the liquid phase filtrate specific conductivity, using a high frequency Wheatstone bridge described below.

5. Wheatstone Bridge

A highly accurate 1000 - 3000 cps Wheatstone bridge was used to measure both streaming potential cell resistance and conductivity cell conductances. It was a model RC - 18 built by Beckman Instruments, Inc., Cedar Grove, N.J. Provisions for balancing the cell lead capacitance were provided.

6. pH Meter

pH Measurements were carried out using a Beckman Zeromatic pH meter (Beckman Instruments, Inc., Cedar Grove, N.J.) with calomel and pH electrodes and suitable calibration buffer solutions.

7. Electrometer

A high imput impedance (10^{-4} ohm) electrometer (Model 610B of Keithley Instruments, Inc., Cleveland, Ohio) was used to measure streaming potentials. The high impedance allowed negligible current to flow across the Ag,AgCl

electrode-liquid interface thereby suppressing electrode polarization during DC measurements.

8. Pressure Transducers

A pair of bucking-wired linear pressure transducers (Automatic Timing and Controls, King of Prussia, Pa.) was connected to the pressure and vacuum sides of the streaming apparatus. Output from the accompanying activator-demodulator was fed to an x-y plotter together with the electrometer output.

9. x - y Plotter

An x - y plotter (Electronic Associates, Inc., N.J.) was used to simultaneously record streaming potential and forcing pressure difference across the streaming potential cell.

10. Andreasen Pipettes

A specially designed pipette (see Figure 10) was used to measure Stokes' law radii as a function of cummulative weight percent of settled solids. This pipette is available from Fisher Scientific, New York. A modified version of this apparatus was set up as shown in Figure 11. The overall height was increased by a factor of four so as to be able to make measurements for flocculation systems of larger particle size than handled by the standard pipette (107).

Figure 10

Andreasen Pipette

Note: This specialized settling rate apparatus is available from Fisher Scientific Co.

Note: reference (107)

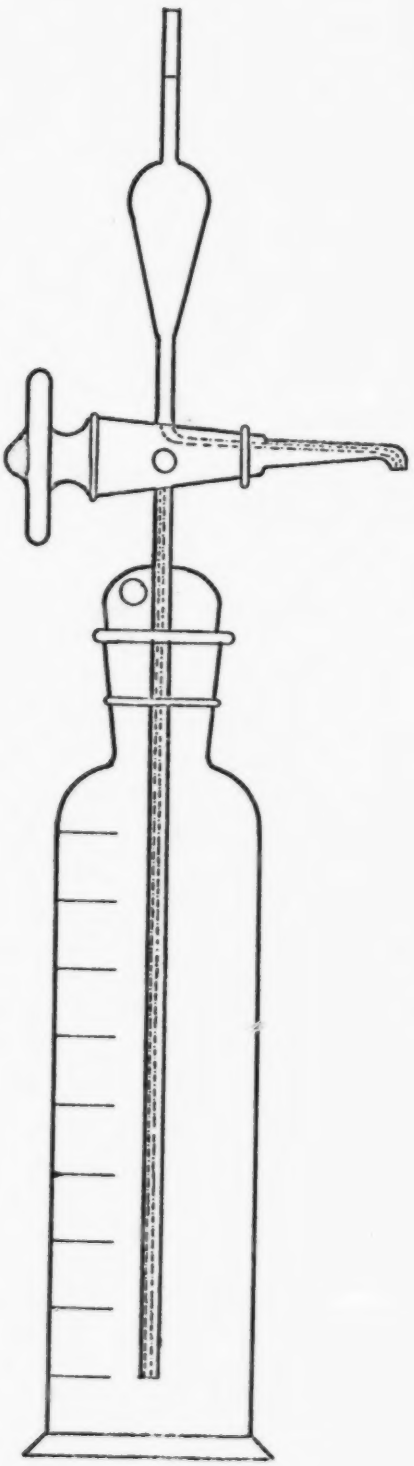

Figure 11

Large Settling Pipette With Enclosure

A top portion of the Andreasen pipette (see Figure 11)

B 100 cm length of 2 inch glass tubing

C fine bore capillary tubing

D wall

E enclosure whose purpose is to reduce temperature gradients caused by air currents in the room

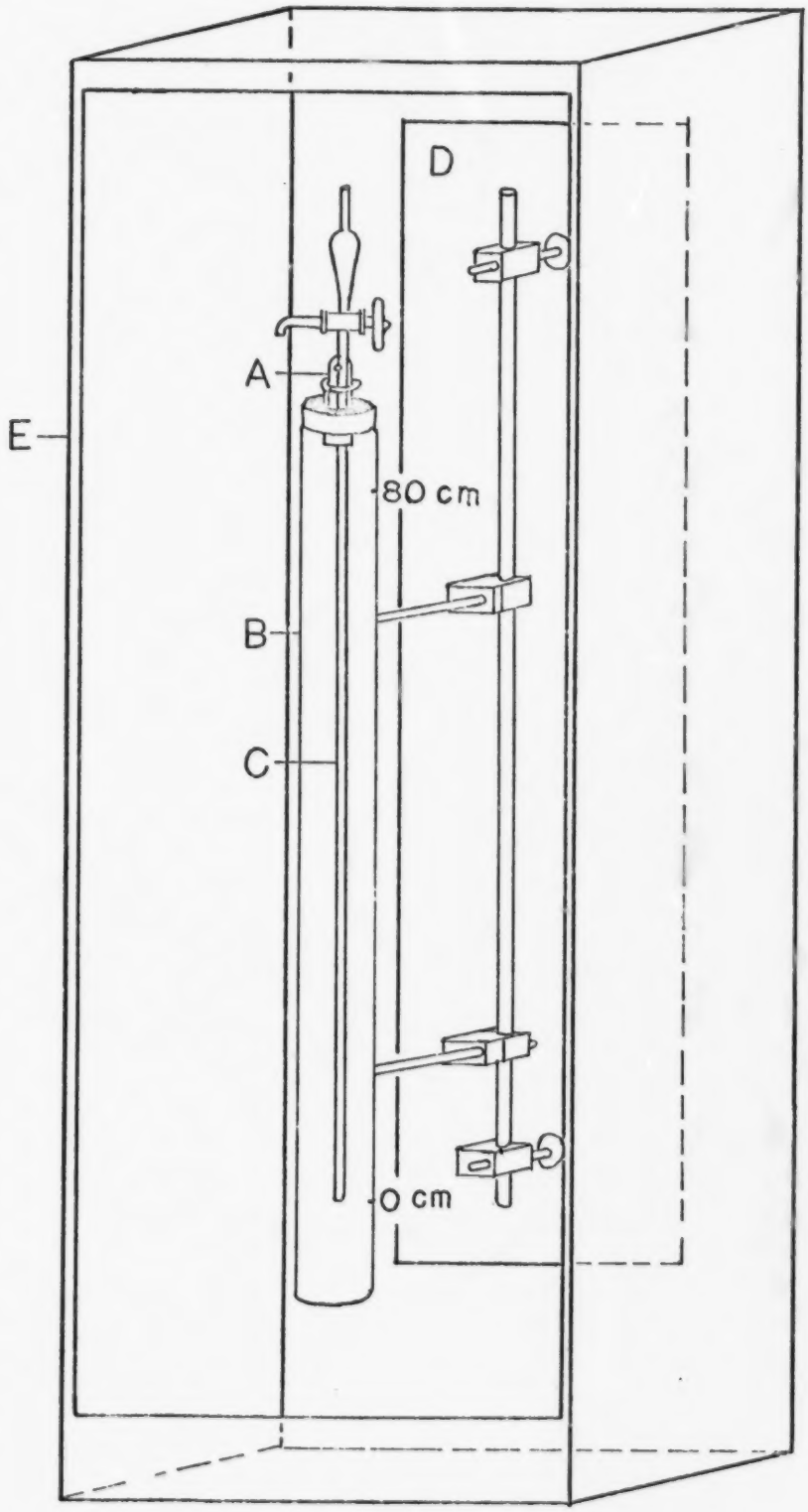
D
A
E
80 cm
B
C
0 cm

C. Procedure

The experimental work consisted of the study of a matrix of flocculation systems as shown in Table 1. Vertically the amount of variation of added PEI flocculant was varied, and horizontally KCl electrolyte content was varied.

Each 100 cc system of the matrix was prepared as follows. To 50 cc of water sufficient 5 micron nominal Min-U-Sil (primary silica) and sufficient concentrated aqueous KCl were added so that at the final 100 cc system volume of the system there would be 0.4 st% primary silica and the correct KCl concentration. This suspension was stirred in a beaker for five minutes with a magnetic stirrer at a constant rate using a teflon coated magnetic stirring bar. To a second 50 cc of water, sufficient aqueous PEI (polyethylcneimine) solution was added so that the final 100 cc system volume would contain the correct PPM of PEI. This dilute PEI was added to the primary silica suspension at a constant rate (2.5 cc/sec) through a suitable charging funnel. Stirring was maintained during PEI addition. The resulting 100 cc flocculation system was stirred five minutes. Effect of PEI addition rate on refiltration rate studies has been shown to be small (108). However, too fast a rate of addition has been found to lead to non-equilibrium adsorption and thus to a variation in resulting surface charge density (109). The constant rate used merely was taken as a precaution to give better precision in the subsequent streaming potential (electrokinetic) measurements.

Table 1

Flocculation Systems Matrix

PPM PEI	10^{-4} NKCl	10^{-3} NKCl	10^{-2} NKCl
0.0	x	x	
0.1		x	x
0.2	x	x	x
0.4	x		
0.5		x	x
0.6	x		
0.8	x		
1.0	x	x	x
1.2	x		
1.3		x	x
1.4	x		
1.6	x	x	x
1.8	x		
2.0	x		
2.2	x		
2.4	x	x	
2.6			x
3.0	x	x	

The completed system was then transferred by fast suction, using house vacuum, to the filtration flask shown in Figure 12. The bottom half of a streaming cell (see Figure 7), (which upon complete assembly consists of two Ag,AgCl electrodes above and below the packed bed of flocculated solids), with the bottom Ag,AgCl electrode, was attached to the bottom of the filtration flask (see Figure 12). A tared 1.2 μ Millipore filter support was clamped between the two precision ground glass surfaces of this bottom half of the streaming potential cell (see Figure 12) so that the filter support fell immediately on top of the bottom Ag,AgCl electrode. When the filtration apparatus was fully assembled (see Figure 12) the flocculation system was filtered under 74 cm Hg vacuum so that a filter bed of flocs was built up on top of the filter support. When filtration was nearly complete (care being taken not to suck the bed dry), an aliquot of clear filtrate was removed and refiltered through the bed. The corresponding constant rate of refiltration was measured. To achieve accuracy, the filtration flask was replaced by a modif'ed buret as the supply of clear filtrate during refiltration (see Figure 13). Buret and time readings allowed an assessment of the refiltration rate. Vacuum was released and the pH and specific conductivity of the remaining filtrate were measured. No attempt was made to adjust pH since primary interest was in keeping the conductivity at a constant level for a given vertical set of runs (see Table 1). Measured pH variation was not great considering such an unbuffered

Figure 12

Filtration and Refiltration Apparatus

A filtration flask

B bottom part of the streaming cell

C vacuum breaker

D filtrate collection flask

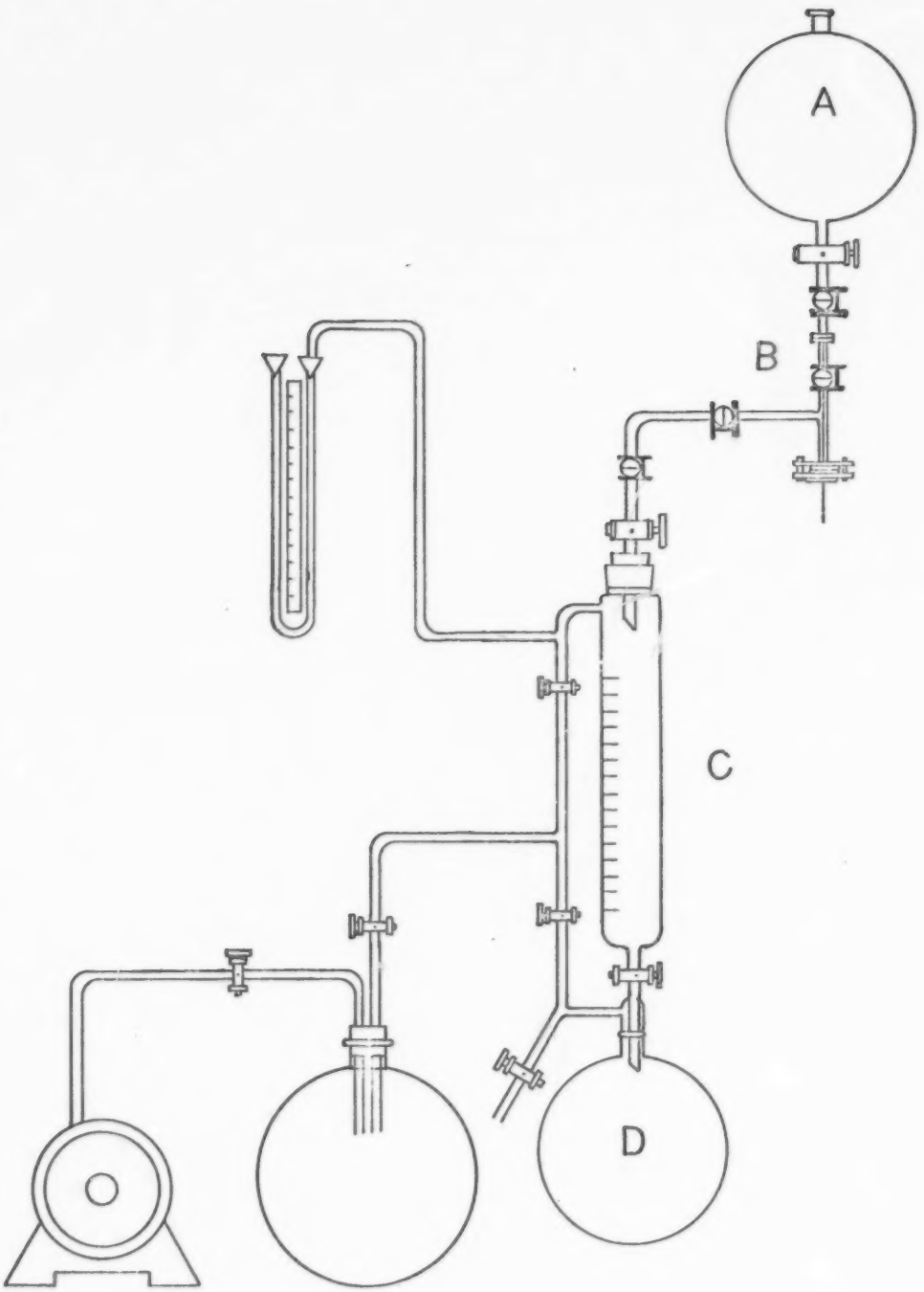
A
B
C
D

Figure 13

Refiltration Apparatus Using Buret
As Filtrate Supply

A buret tube

B bottom part of streaming cell

C vacuum breaker

D filtrate collection flask

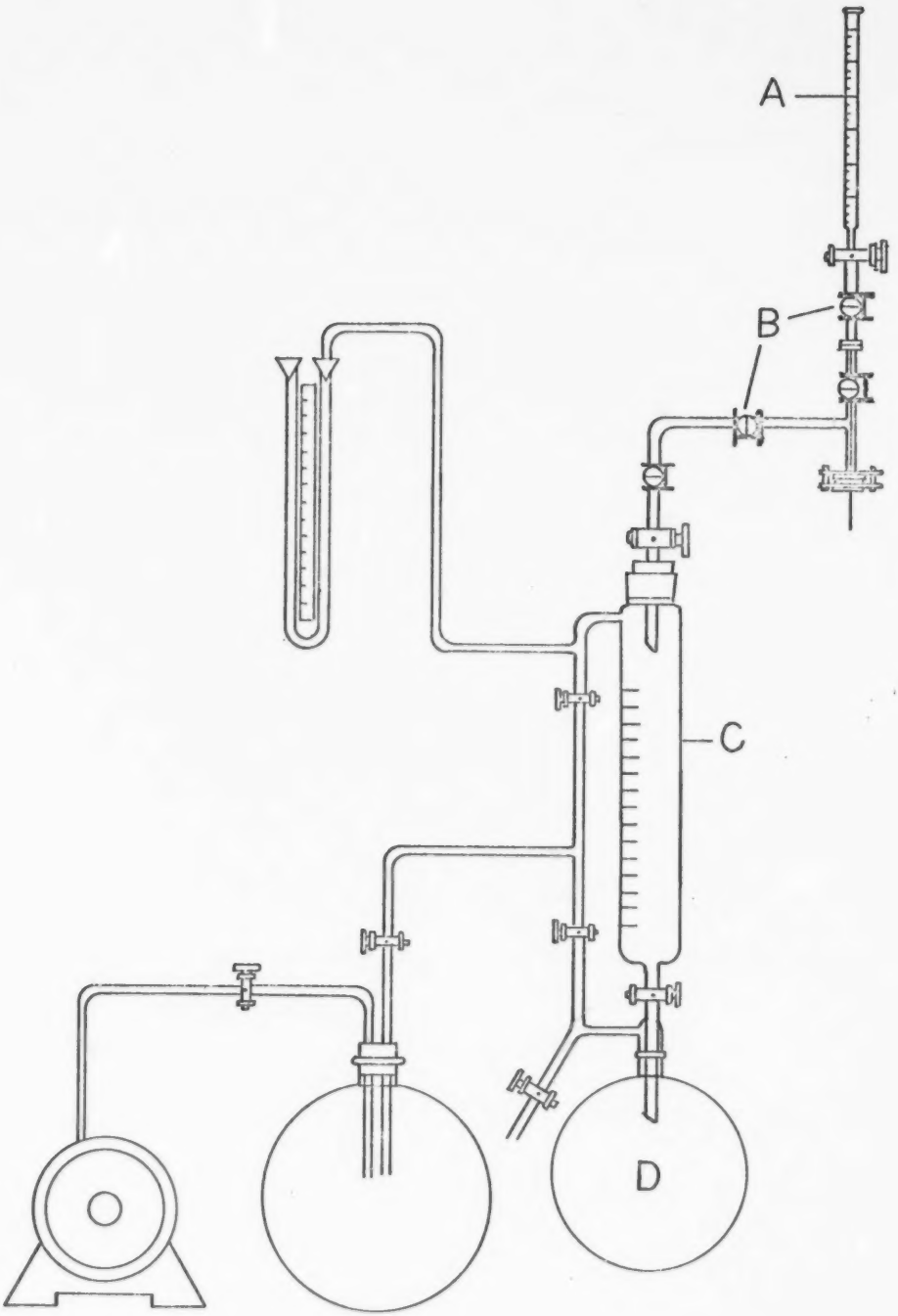
A
B
C
D

set of systems.

After refiltration measurements, the bottom half of the streaming potential cell was disconnected from the filtration apparatus and, together with the contained floc bed, was transferred and connected to the streaming potential apparatus as shown in Figure 8. The complete streaming potential cell was assembled with Ag,AgCl electrodes on top and below the floc bed. The top movable electrode, attached to the Starret micrometer, (see Figure 7) was adjusted to the top of the floc bed in the streaming potential cell, so that the bed depth could be calculated from the micrometer reading and a previously taken zero depth reading.

The leads of the 610B Keithley electrometer were attached to the Ag,AgCl electrodes of the streaming potential cell. In order to collect a sufficient volume of filtrate to use as the streaming medium, a separate proportionately larger 1000 cc flocculation system was prepared in the same manner as the 100 cc system and fast filtered through a large Buchner type funnel. This filtrate was forced under vacuum to flow through the assembled streaming potential cell from the left hand 1 liter reservoir to the right hand 1 liter reservoir of the streaming potential apparatus (see Figure 8). Both the developed streaming potential, E_s, and the forcing pressure difference, $\triangle P$, were recorded for a series of pressure differences on an x - y plotter so that the slope of the plot could be used as a measure of $(E_s / \triangle P)$. A calibrated set of bucking - wired linear pressure transducers

provided the pressure difference signal to the plotter. Streaming was stopped by slowly releasing the forcing pressure difference (so as to maintain liquid in the floc bed). The resistance of the complete assembled streaming potential cell (including the floc bed) was measured using a high frequency AC Wheatstone bridge. An attempt was made to directly measure the streaming current as a function of the forcing pressure difference by using the 610B Keithley electrometer as a fast balancing zero resistance ammeter. An x - y plot of this measured value of I vs. $\triangle P$ was recorded.

With the electrokinetic data taken, the streaming potential cell was disassembled. The floc bed porosity was determined by carefully taking wet and dry weights of the bed. The pH and specific conductivity of the filtrate used as the "streaming medium" were measured. Room temperature, barometric pressure and static head between the right and left hand streaming medium reservoirs were recorded.

The cumulative wt% settled particle size distribution for a given system was determined on separate preparations using a modified version of the Andreasen pipette (Fisher Scientific, N.Y.) (see Figures 10 and 11). Measurements were carried out following a method described by Loomis (110). The height of the sampling point from the top of the liquid and the time since the halt of mixing were recorded for a series of 10 cc samples. Weights of the dried samples and calculation of Stokes' radii (111) allowed a

plot of the cumulative wt% particle size distribution. The implicit assumption of pure silica flocs was made. Using a log probability grid the geometric mean and the geometric standard deviation of particle size were determined for each system. Calculation of d_{sv} from these two parameters was then straight forward (112). The measurements were carried out only at the 10^{-4} N KCl level and only at selected PEI concentrations.

V. Results of laboratory measurements

A. Tabulation of Results

Table 2

Key:

RUN: xp00qrKs
x denotes cell #PN
p denotes run subnumber
qr denotes q.r PPM PEI

RFR: refiltration rate, ml/min

$\triangle$Pf: filtration vacuum, cm Hg

FpH: filtrate pH

$dE/d\triangle P$: slope of E_s vs. $\triangle P$ plot, mv/cm Hg

$dI/d\triangle P$: slope of I vs. $\triangle P$ plot, 10^{-4} ma/cm Hg

R_{bridge}: cell resistance measured by A.C. bridge, ohms

f: bridge frequency, Kc

d_B: depth of floc bed, cm

ϵ: floc bed porosity

SMpH: streaming medium pH

SMλ: Streaming medium specific conductivity, 10^{-6} mhos/cm

Note: PEI is the abbreviated name for ET 723, a Dow Chemical Co. polyethyleneimine.

RUN	RFR	△Pf	FpH	dE/d△P	dI/d△P	R_{bridge}	f	d_B	∈	SMpH	SMλ
10002K4	0.58	74.5	6.1	6.43	1.29	40680	1	0.576	0.67	6.3	18.5
x20002K4	0.67	73.5	6.0	6.23	1.47	39900	1	0.535	0.67	6.2	19.2
30002K4	0.57	74.7	6.2	6.17	1.32	42400	1	0.551	0.67	6.3	18.3
x10004K4	0.79	74.8	6.3	6.53	1.15	48032	1	0.597	0.70	6.3	18.1
20004K4	0.70	74.5	6.4	6.37	1.09	49600	1	0.617	0.68	6.2	18.5
x30004K4	0.67	74.5	6.3	6.13	1.28	41430	1	0.556	0.69	6.3	19.8
10006K4	0.75	74.5	6.3	5.53	0.850	60300	1	0.642	0.68	6.3	18.2
x20006K4	0.81	74.5	6.2	5.37	0.840	56820	1	0.632	0.69	6.3	18.5
30006K4	0.65	75.4	6.3	5.40	0.913	53600	1	0.559	0.67	6.4	18.0
10008K4	0.77	75.5	6.2	4.17	0.643	60600	1	0.627	0.68	6.2	18.6
x20008K4	0.85	75.5	6.0	3.90	0.667	57000	1	0.576	0.69	6.3	18.3
30008K4	0.72	76.2	6.7	4.17	0.713	52120	1	0.508	0.69	6.4	18.7
10010K4	0.77	75.9	6.2	2.50	0.383	49700	1	0.541	0.70	6.2	18.9
x20010K4	0.77	75.3	6.2	2.37	0.327	61450	1	0.619		6.2	18.9
30010K4	0.78	75.7	6.4	2.63	0.377	56500	1	0.566	0.70	6.3	19.5
x10012K4	0.82	75.2	6.0	0.933	0.147	53200	1	0.551	0.69	6.3	18.6
20012K4	0.73	75.7	6.4	0.767	0.107	62700	1	0.579	0.70	6.2	18.7
x30012K4	0.78	75.7	6.2	0.967	0.143	58460	1	0.561	0.69	6.3	19.6
10014K4	0.78	76.0	6.2	-1.07	-0.140	68500	1	0.579	0.70	6.3	18.9
x20014K4	0.80	73.2	6.2	-0.633	-0.0767	71000	1		0.69	6.0	18.7
30014K4	0.72	73.0	6.0	-0.567	-0.0733	69600	1	0.571	0.70	6.1	19.7

RUN	RFR	ΔPf	FpH	dE/dΔP	dI/dΔP	R_{bridge}	f	d_B	ϵ	SMpH	SMλ
x10016K4	0.80	74.5	6.2	-2.20	-0.313	59200	1	0.518	0.70	6.2	19.7
20016K4	0.79	75.0	6.5	-2.17	-0.300	65000	1	0.520	0.69	6.4	20.1
60016K4	0.83	74.2	6.1	-2.30	-0.253	70000	1	0.589	0.73	6.2	19.0
10018K4	0.76	74.4	6.2	-3.80	-0.483	69100	1	0.551	0.73	6.3	19.0
x20018K4	0.80	74.4	6.2	-3.87	-0.550	62500	1	0.490	0.71	6.2	19.8
30018K4	0.74	74.4	6.2	-3.63	-0.490	67600	1	0.538	0.71	6.2	20.3
x10020K4	0.74	74.0	6.3	-5.70	-0.800	65300	1	0.503	0.72	6.3	20.1
20020K4	0.73	74.0	6.4	-5.63	-0.823	69200	1	0.541	0.72	6.4	20.4
x30020K4	0.76	74.0	6.4	-5.10	-0.757	62300	1	0.495	0.73	6.3	20.3
10022K4	0.66	75.0	6.4	-7.20	-0.930	72420	1	0.520	0.72	6.4	18.9
x20022K4	0.75	74.7	6.4	-6.80	-0.787	68700	1	0.472	0.70	6.4	18.8
30022K4	0.69	74.5	6.4	-7.37	-0.935	71660	1	0.525	0.72	6.4	19.2
10024K4	0.68	74.8	6.5	-8.10	-1.090	67700	1	0.477	0.71	6.4	18.6
20024K4	0.71	74.6	6.2	-7.60	-1.080	67600	1	0.490	0.72	6.2	19.4
x30024K4	0.72	75.2	6.4	-7.70	-1.130	62250	1	0.442	0.69	6.2	19.6
10030K4	0.60	75.9	6.5	-8.70	-1.200	65470	1	0.497	0.71	6.2	19.6
x20030K4	0.66	75.8	6.6	-8.40	-1.190	64970	1	0.505	0.70	6.5	20.3
30030K4	0.65	75.5	6.3	-8.30	-1.160	67312	1	0.508	0.71	6.4	19.8
x10000K4	0.18	75.8	6.1	+5.00	+1.600	23340	1	0.289	0.68	5.9	16.5

RUN	RFR	△Pf	FpH	dE/d△P	dI/d△P	R_{bridge}	f	d_B	∈	SMpH	SMλ
10001K3	0.61	74.9	6.0	2.42	2.23	8593	3	0.440	0.70	6.0	139.8
10002K3	0.66	74.9	6.2	2.15	1.92	9136	3	0.548	0.70	6.3	155.0
10005K3	0.81	74.9	6.3	1.63	1.54	9416	3	0.542	0.69	6.2	154.0
10010K3		74.5	6.3	0.85	0.648	10695 10890	3 1	0.554	0.71	6.3	152.0
10013K3	0.83	74.5	6.3	0.180	0.163	9569 9657	3 1	0.498	0.73	6.3	151.0
10016K3	0.80	73.9	5.8	-0.320	-0.227	11030 11120	3 1	0.582	0.72	6.3	151.0
10024K3	0.73	74.9	6.4	-1.530	-1.313	10072 10132	3 1	0.465	0.70	6.4	146.0
10030K3	0.62	74.0	6.8	-1.760	-1.570	10947 10991	3 1	0.465	0.71	6.3	149.0
10000K3	0.21	74.0	6.1	+2.47	+2.37	7916 8081	3 1	0.272	0.66	5.8	180.0

RUN	RFR	$\triangle$Pf	FpH	dE/d$\triangle$P	dI/d$\triangle$P	R_{bridge}	f	d_B	ϵ	SMpH	SMΛ
x10001K2	0.61	74.0	6.1	0.265	0.74	1196 1205	3 1	0.465	0.72	5.9	1482
10002K2	0.65	75.4	5.8	0.288	1.17	1404 1414	3 1	0.563	0.72	5.9	1310
x10005K2	0.72	74.6	5.8	0.193	0.70	1380 1389	3 1	0.510	0.72	6.2	1280
10010K2	0.75	74.0	-	0.082	0.192	1107 1116	3 1	0.619	0.73	-	1755
x10013K2	0.74	74.3	6.2	0.00	0.00	1372 1381	3 1	0.530	0.74	6.3	1320
10016K2	0.84	74.1	6.3	-0.036	-0.167	1393 1402	3 1	0.614	0.73	5.8	1410
x10026K2	0.83	73.0	6.7	-0.140	-0.510	1289 1298	3 1	0.470	0.71	6.4	1313
x10030K2	0.70	75.00	6.8	-0.160	-0.490	1330 1341	3 1	0.498	0.73	6.4	1325

B. Refiltration rates

Figure 14 shows a plot of refiltration rate as a function of PPM PEI for the experimental matrix of Table 1.

C. Particle size measurements

The results of statistical analysis of the Stokes' law settling rate studies carried out with the Andreasen pipettes are shown plotted as surface-volume mean diameter d_{sv} against PPM PEI in Figure 15.

D. Zeta potential calculations

I. Zeta potential calculations from streaming potential data ignoring effect of surface conduction.

Figure 16 shows the apparent Zeta potentials calculated from streaming potential data i.e., from η, D, λ, and $(E_s/\Delta P)$. Note that bulk liquid phase specific conductivities, λ, were used here. It has been assumed that the slopes, $dE/d\Delta P$, of the experimental plots equal the ratio $(E_s/\Delta P)$ thereby accounting for the effect of nonequipotential Ag,AgCl electrodes at zero ΔP. The equation used is then

$$ZPA = [(4\pi\eta)/D] \cdot (E_s/\Delta P) \cdot \lambda \qquad [36]$$

where ZPA signifies the apparent Zeta potential.

Figure 14

RFR vs. PPM PEI for 0.4 wt% silica

RFR	refiltration rate
PEI	polyethyleneimine (ET723)

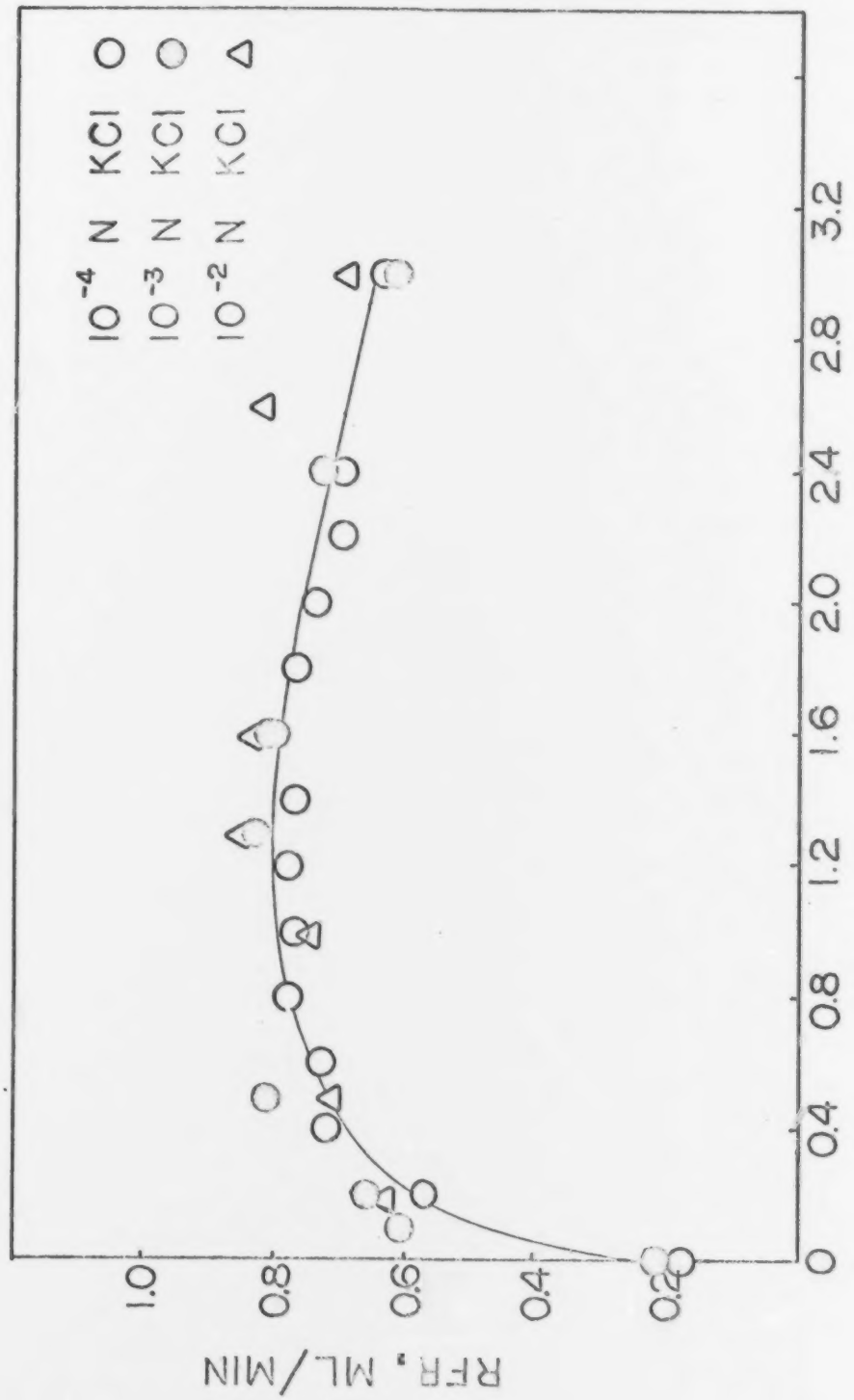
10^{-4} N KCl
10^{-3} N KCl
10^{-2} N KCl
RFR, ML/MIN
1.0
0.8
0.6
0.4
0.2
0
0.4
0.8
1.2
1.6
2.0
2.4
2.8
3.2
PPM PEI

Figure 15

d_{sv} vs. PPM PEI for 0.4 wt% silica

d_{sv}	surface-volume mean particle diameter
PEI	polyethyleneimine (ET723)

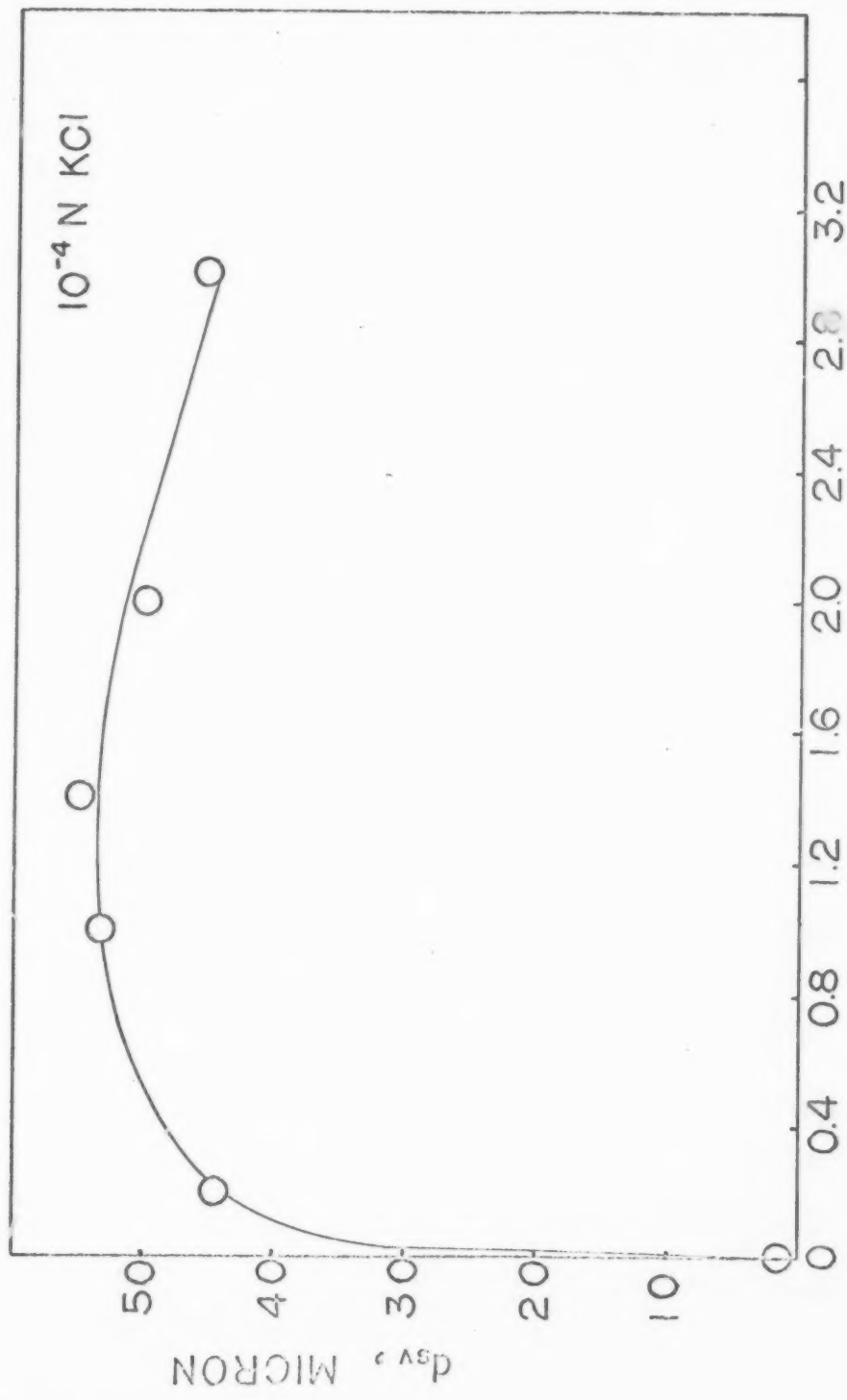
10^{-4} N KCl
d_{sv}, MICRON
50
40
30
20
10
0
0.4
0.8
1.2
1.6
2.0
2.4
2.8
3.2
PPM PEI

Figure 16

ZPA vs. PPM PEI for 0.4 wt% silica

ZPA	Zeta potential calculated from bulk value of specific conductivity λ
PEI	polyethyleneimine (ET723)

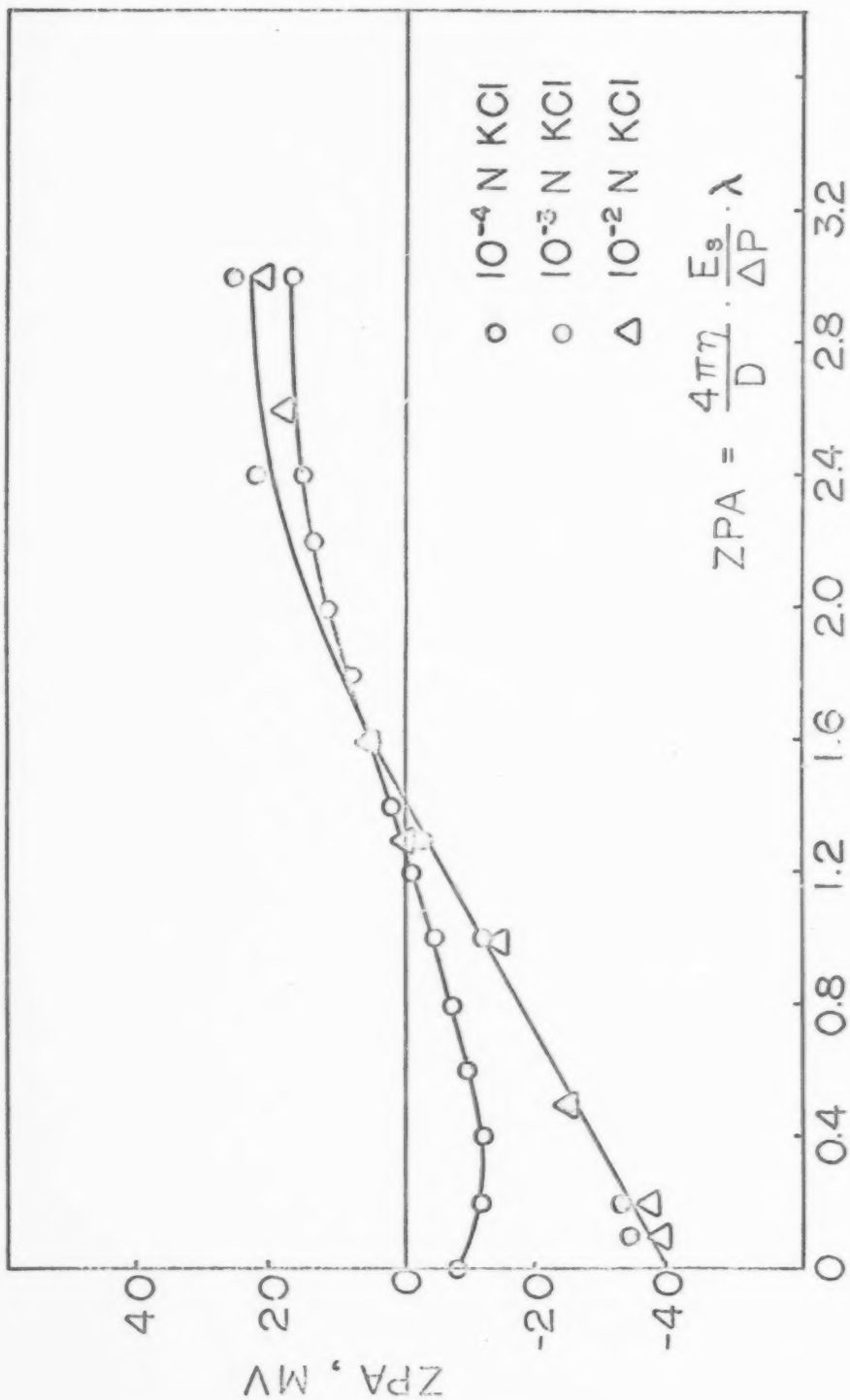
ZPA , MV
40
20
0
-20
-40
0
0.4
0.8
1.2
1.6
2.0
2.4
2.8
3.2
PPM PEI
o 10^{-4} N KCl
o 10^{-3} N KCl
Δ 10^{-2} N KCl
$ZPA = \frac{4\pi\eta}{D} \cdot \frac{E_s}{\Delta P} \cdot \lambda$

2. Streaming current data and "EKCF"

Figure 17 shows a plot of the parameter $(-d_B)[(E_s/\triangle P)/R_{bridge}]$ vs PPM of PEI where $(-d_B)[(E_s/\triangle P)/R_{bridge}]$ is called the electrokinetic control function "EKCF". Here d_B is the micrometer-measured floc bed depth, E_s is the streaming potential, $\triangle P$ is the forcing pressure difference and R_{bridge} is the resistance of the floc-filled streaming potential cell. It is to be expected that this parameter should behave the same as the Zeta potential calculated from streaming potential data with the effect of surface conduction accounted for. For replicate runs on any <u>one given system</u>, the effective area of the floc bed perpendicular to liquid flow should be the same for a given streaming potential cell (i.e. the cell without the floc bed) whose overall cross-sectional A_c is constant. The cell constant, K, of such a floc-filled cell should be relatable to d_B/A_c and hence $(-d_B)[(E_s/\triangle P)/R_{bridge}]$, i.e., "EKCF", should be related to $(K)[I_s/\triangle P]$ where the streaming current $I_s = E_s/R_{bridge}$. Again it has been implicitly assumed that $E_s/\triangle P = dE/d\triangle P$.

Calculation of (d_B/K_a) where d_B is the measured floc bed depth and where K_a is an apparent cell constant, i.e., $K_a = \lambda R_{bridge}$, shows that (d_B/K_a) remains constant for replicate runs on a particular member system of the Table 1 matrix. Letting (d_B/K_a) represent an apparent effective cross-sectional area, A_E, of the floc bed, Figure 18 shows

Figure 17

EKCF vs. PPM PEI for 0.4 wt% silica

EKCF	empirical electrokinetic control function
PEI	polyethyleneimine (ET723)

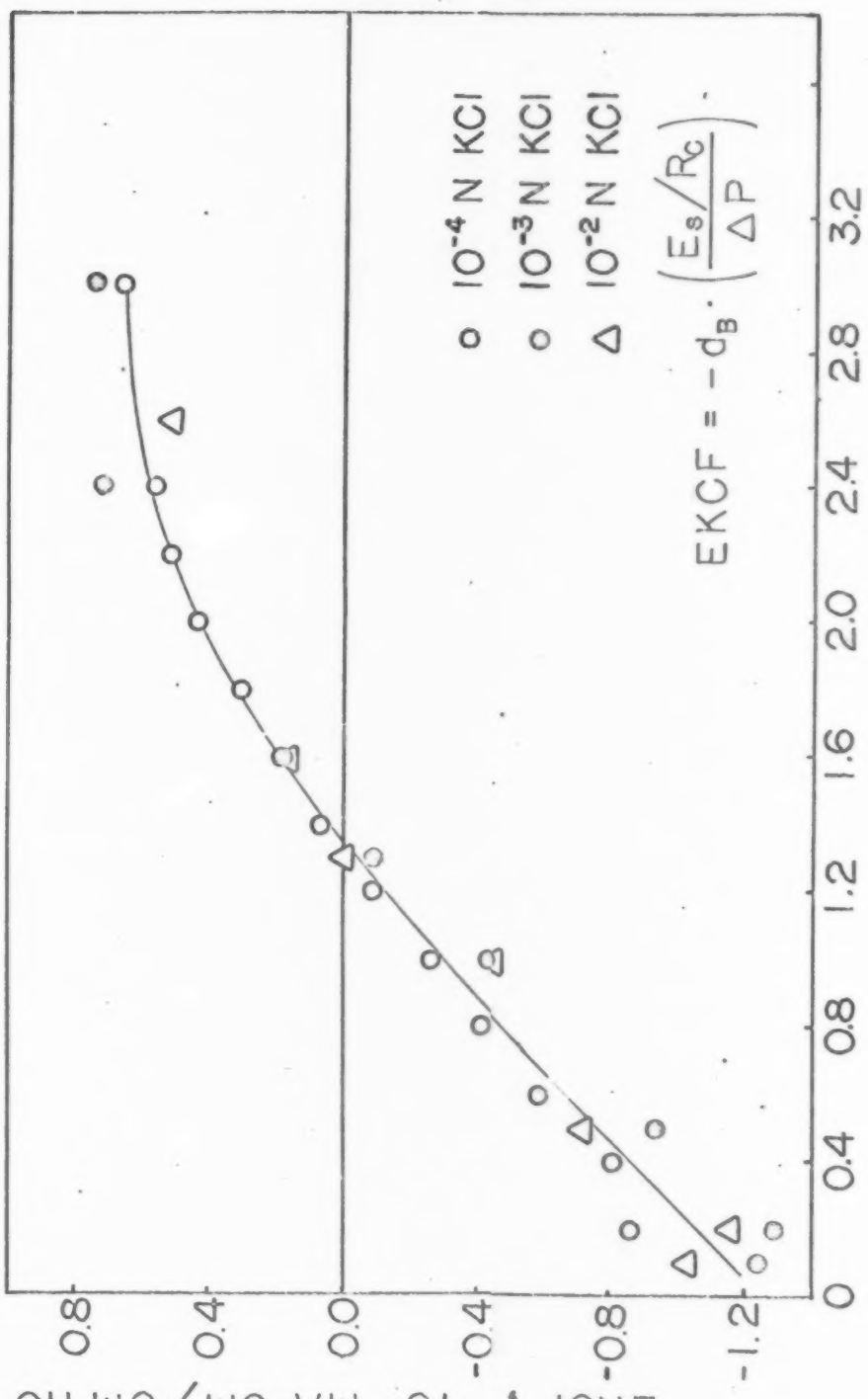
EKCF , 10^{-4}MA-CM/CM HG
0.8
0.4
0.0
-0.4
-0.8
-1.2
0
0.4
0.8
1.2
1.6
2.0
2.4
2.8
3.2
PPM PEI
10^{-4} N KCl
10^{-3} N KCl
10^{-2} N KCl
$EKCF = -d_B \cdot \left(\frac{E_s/R_c}{\Delta P}\right)$

Figure 18

A_E vs PPM PEI for 0.4 wt% silica

A_E apparent effective area

PEI polyethyleneimine (ET723)

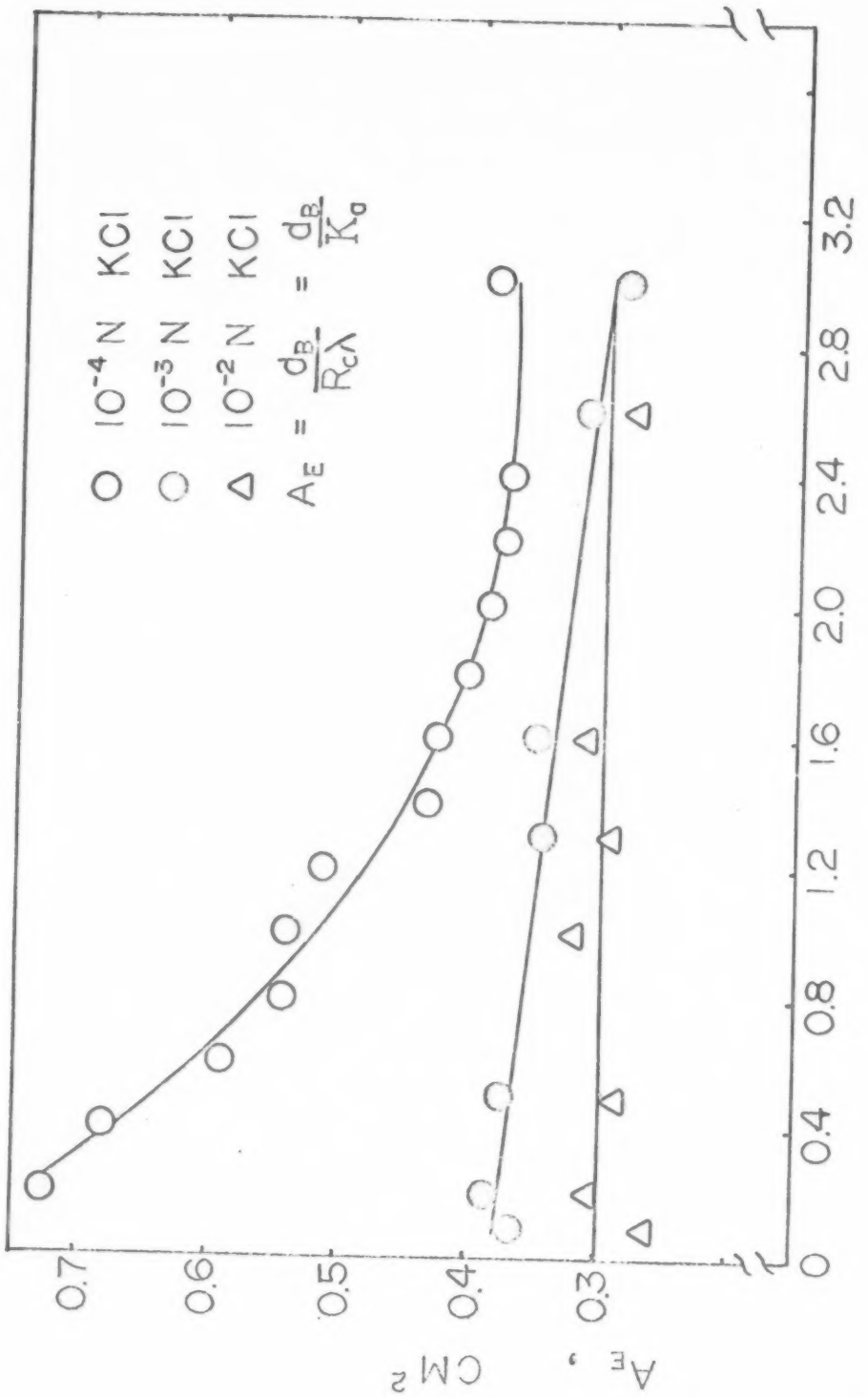
10^{-4} N KCl
10^{-3} N KCl
10^{-2} N KCl
$A_E = \frac{d_B}{R_c\lambda} = \frac{d_B}{K_o}$
A_E , CM^2
0.7
0.6
0.5
0.4
0.3
0
0.4
0.8
1.2
1.6
2.0
2.4
2.8
3.2
PPM PEI

A_E plotted against PPM PEI for each of the KCl levels. Note that at 10^{-2} N KCl a straight horizontal line is drawn denoting independence of $A_E = d_B/K_a$ from PPM PEI at this high KCl level. Variation of the A_E- PPM PEI line from this horizontal at the other lower KCl levels points out the effect of surface conduction at the 10^{-3} and 10^{-4} N KCl levels. It was then possible for example to use the ratio of A_E at 10^{-4} N KCl to A_E at 10^{-2} N KCl, for a set value of PPM PEI, to correct the apparent Zeta potential for the surface conduction effect. Letting ZPC be the corrected Zeta potential then for the 10^{-4} N KCl level,

$$ZPC = ZPA \quad \frac{(A_E)_{@10^{-4}\ N\ KCl}}{(A_E)_{@10^{-2}\ N\ KCl}} \qquad [37]$$

similar relationships were set up for all Table 1 matrix members so that corrected Zeta potentials were calculated for all 10^{-4} and 10^{-3} N KCl members based on the corresponding 10^{-2} N KCl member at each PPM PEI vertical matrix level. ZPC is shown in Figure 19 plotted against PPM PEI.

E. Specific surface conductivity calculations

Employing the expression developed in the theory chapter namely,

$$\chi = [(K/K_a) - 1] \cdot [\epsilon/(1-\epsilon)] \cdot [d_{sv}/6] \cdot [\lambda] \qquad [38]$$

values of the specific surface conductivity, χ, were calculated for each of the members of the 10^{-3} and 10^{-4} N KCl levels of the Table 1 experimental matrix, based on cell

Figure 19

ZPC vs. PPM PEI for 0.4 wt% silica

ZPC	Zeta potential corrected for surface conduction effect
PEI	polyethyleneimine (ET723)
A_E	apparent effective area (see figure 18)
$(A_E)_{K2}$	corresponding effective area at 10^{-2} N KCl level (see figure 18)
K2	signifies 10^{-2} N KCl

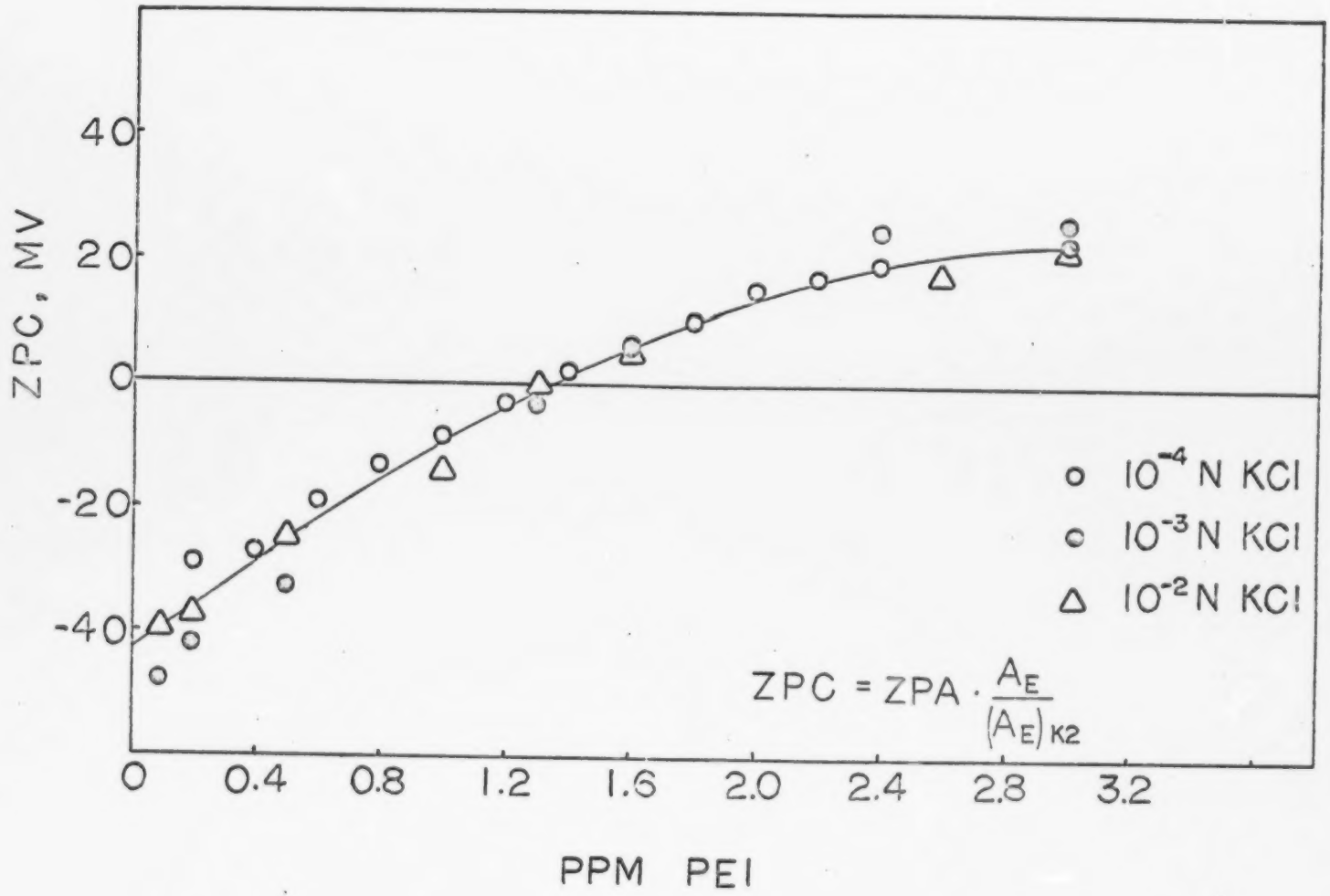
ZPC, MV
40
20
0
-20
-40
0
0.4
0.8
1.2
1.6
2.0
2.4
2.8
3.2
PPM PEI
10^{-4} N KCl
10^{-3} N KCl
10^{-2} N KCl
$ZPC = ZPA \cdot \frac{A_E}{(A_E)_{K2}}$

constants, K, calculated from

$$K = d_B \left(\frac{1}{A_{E\ @10^{-2}\ N\ KCl}} \right) \qquad [39]$$

It was assumed that surface conductance C_s was a small fraction of total conductance C_c at the 10^{-2} N KCl level. The results are plotted in Figure 20 as a function of PPM PEI. Overbeek (113) notes that χ is proportional to the square root of the bulk electrolyte concentration. Therefore to check the above assumption that C_s is a minor fraction of C_c, or alternately that $\frac{\chi}{r_H}$ is a minor fraction of λ_c, a line representing χ as a function PPM PEI was calculated for the 10^{-2} N KCl level by extrapolation from the 10^{-3} and 10^{-4} N KCl lines of Figure 20. Calculation of the net effective specific conductivity, λ_c, was made as follows,

$$\lambda_c = \lambda + (\chi / r_H) \qquad [40]$$

where r_H is the hydraulic radius of a given floc bed. The contribution of surface conductance to effective specific conductivity was obtained for the systems studied. Results are shown for 0.2 PPM PEI in Table 3. These are about the maximum surface conduction contributions for each level of KCl. Therefore the maximum contribution at the 10^{-2} N KCl level was 7%. Hence the assumption of a small surface conduction contribution at 10^{-2} N KCl is valid for the systems studied.

Figure 20

χ vs. PPM PEI for 0.4 wt% silica

χ	specific surface conductivity
PEI	polyethyleneimine (ET723)
N	normality of KCl

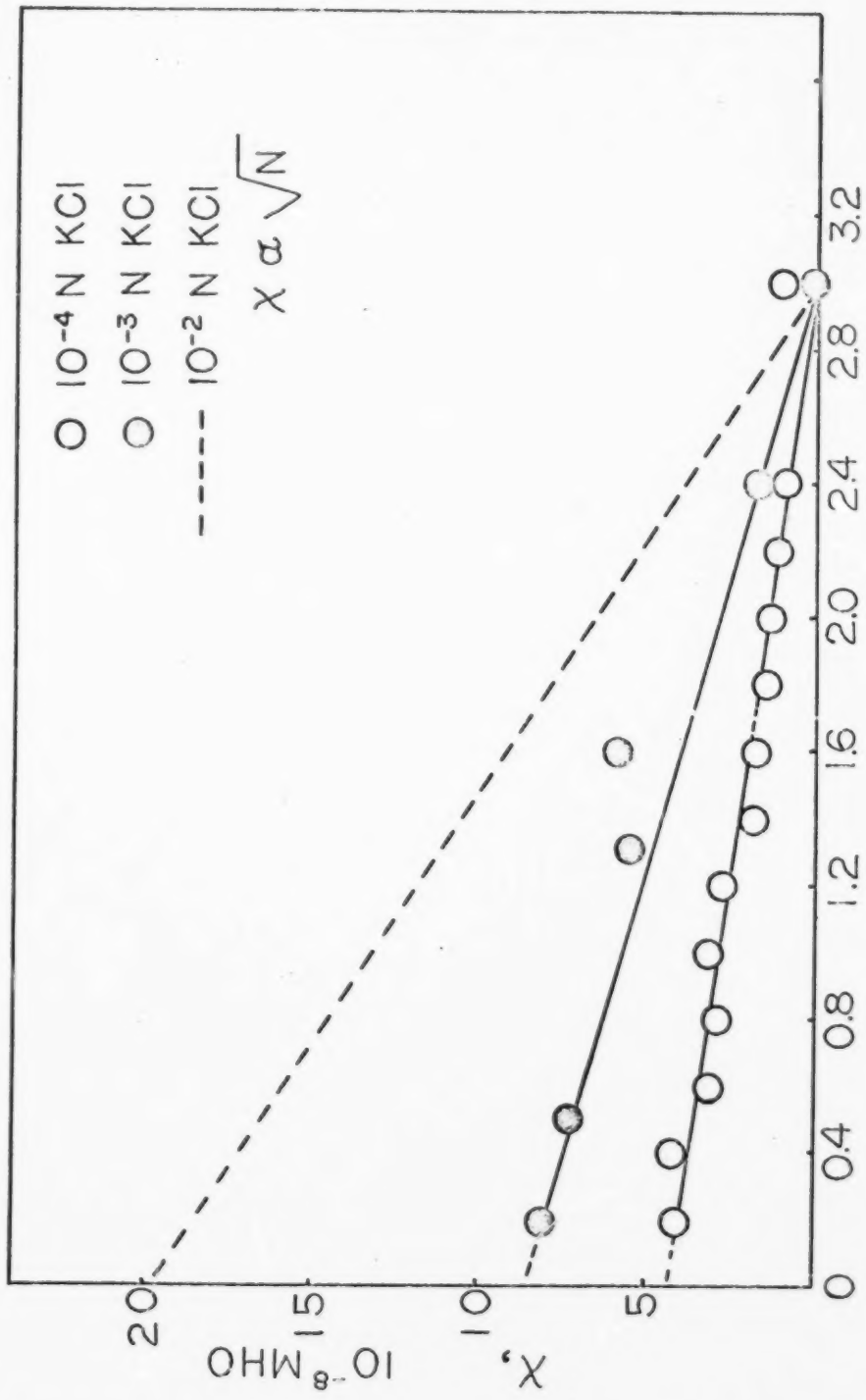
O 10⁻⁴ N KCl
O 10⁻³ N KCl
---- 10⁻² N KCl
χ α √N
χ, 10⁻⁸ MHO
20
15
10
5
0
0
0.4
0.8
1.2
1.6
2.0
2.4
2.8
3.2
PPM PEI

Table 3

N KCl	μmho/cm λ	μmho/cm χ/r_H	μmho/cm λ_c	% = $100[1-(\lambda/\lambda_c)]$
10^{-4}	19	27	46	59
10^{-3}	150	46	196	23
10^{-2}	1300	93	1393	7

VI. Discussion of Results

A. Refiltration rate studies

The graphical plots of refiltration rate RFR against the flocculant concentration expressed as PPM PEI, for the 0.4 wt% 5 u silica systems studied, resemble results in the literature (114). Correlation of refiltration rates with Zeta potentials (ZPC) calculated from streaming potential data and corrected for surface conduction shows that the maximum rate of refiltration occurs at 1.2 PPM PEI whereas the zero value of Zeta potential occurs at 1.3 PPM PEI (see Figure 21). This clearly means that control of a given process at zero Zeta potential does not necessarily give the best flocculation effectiveness. In other words, a precise and accurate correlation if required to maintain optimum flocculation. The occurance of the maximum surface-volume mean particle diameter at 1.2 PPM PEI only reinforces the occurance of optimum flocculation at 1.2 PPM PEI.

B. Apparent Zeta Potentials

Calculation of a representative Zeta potential from electrokinetic data was the major aim of the research. Figure 16 shows the apparent Zeta potential, "ZPA", calculated from equation [13] using the bulk value λ of the liquid phase specific conductivity, the surface conduction effect being thus ignored. Clearly ZPA is a function of the KCl concentration. The direction of variation is exactly opposite to the known fact that Zeta potentials are depressed by an increase in KCl concentration in the 10^{-4} to 10^{-2} N KCl range (115). Figure 16 shows

Figure 21

Correlations for 0.4 wt% silica

d_{sv}	surface-volume mean particle diameter
RFR	refiltration rate
ZPC	Zeta potential corrected for surface conduction effect
EKCF	empirical electrokinetic control function equal to $-d_B (E_s/R_c)/\triangle P$
PEI	polyethyleneimine (ET723)
R_c	measured as R_{bridge}

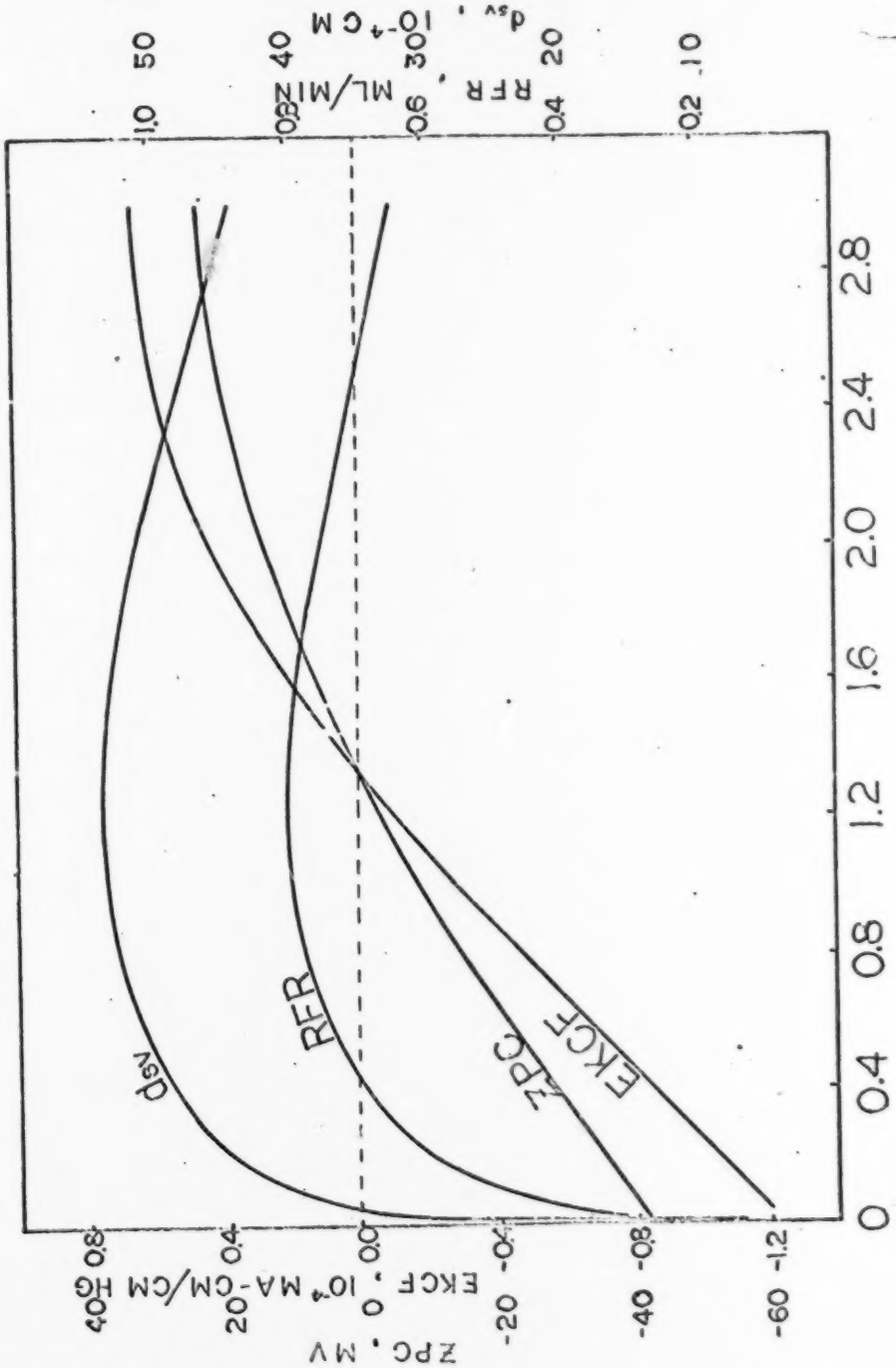
PPM PEI
0
0.4
0.8
1.2
1.6
2.0
2.4
2.8
ZPC, MV
EKCF, 10^{-3} MA-CM/CM HG
0.8
0.4
0.0
-.4
-.8
-1.2
-20
-40
-60
RFR, ML/MIN
.10
.20
.30
.40
.50
d_{sv}, 10^{-4} CM
.02
.04
.06
.08
.10
d_{sv}
RFR
ZPC
EKCF

depression of apparent Zeta potential, ZPA, by a decrease in KCl concentration. This effect led early investigators (116-119) to consider surface conduction. Equation [13] is thus inadequate unless the actual value of the specific conductivity, λ_c, for the liquid in the "capillaries" of the streaming potential cell plug is known.

C. The "EKCF"

"EKCF" is the electrokinetic control function defined as $-d_B[(E_s/R_{bridge}/\triangle P]$. If the analysis given with the presentation of the results is followed, then EKCF should behave the same as ZPC, the Zeta potential calculated from streaming potential data and corrected for the surface conduction effect. Figure 17 definitely shows that EKCF is for practical purposes independent of KCl concentration. Then EKCF can be used in correlation with the refiltration rate to control a flocculation process (see Figure 21). All of the parameters required, i.e., d_B, E_s, R_{bridge} and $\triangle P$ can be obtained directly from laboratory measurements making EKCF a far better candidate than Zeta potential for flocculation process control.

D. Calculated Zeta potential corrected for the surface conduction effect

Figure 19 shows, "ZPC", the calculated Zeta potential corrected for surface conduction, as a function of flocculant concentration. ZPC is for practical purposes independent of KCl concentration. The adequacy of "EKCF" as a process control function is then reinforced since EKCF behaves similar to the surface conduction corrected Zeta potential, ZPC (see Figure 21).

E. The specific surface conductivity χ

Attempts to apply equation [35] are shown in Figure 20. Note that for both 10^{-3} N KCl and 10^{-4} N KCl concentrations the specific surface conductivity, χ, decreases with increase in PPM PEI added. This might indicate that most of the highly mobile ions, i.e., K^+, Cl^-, and H_3O^+, which were originally present as excess charges in the double layer, have been replaced by the cationic high molecular weight PEI molecules. The PEI molecules are certainly not as mobile as K^+, Cl^-, OH^-, H_3O^+ ions, and hence contribute less to surface conduction.

VII. Summary

It was pointed out in the introduction that for flocculation systems similar to those studied here, zero electrophoretic mobility occured at a flocculant concentration near to the concentration which gives optimum flocculation conditions as exhibited by a maximum in the measured rate of refiltration. The difficulties inherent in electrophoretic mobility measurements were discussed in the literature section. Streaming potential measurements were suggested as an alternate electrokinetic means of arriving at an electrokinetic control factor. The present results show that the Zeta potential calculated from streaming potential data using bulk liquid phase properties is not adequate, when the effective specific conductivity of the liquid phase is greater for the liquid in a capillary than for the bulk liquid. This condition can be encountered in potable water supplies. The apparent Zeta potential, ZPA, calculated from η, D, λ, and $E_s/\Delta P$ is then

not the actual Zeta potential when $\lambda<\lambda_c$, λ_c being the effective specific conductivity of the liquid phase in the "capillaries" of the floc bed during the streaming potential measurements. The discrepancy is caused by occurance of surface conduction, i.e., conduction by excess charged particles in the double layer region. λ_c can be determined by measuring the total electrical resistance, R_c, of the streaming potential cell (including the floc bed) and then somehow determining an actual cell constant, K, for this cell, so that λ_c equals (K/R_c).

Laboratory results show that streaming potential can indeed be used as an alternate electrokinetic measurement for calculation of an electrokinetic control factor to be applied to flocculation processes. When the actual cell constant, K, is not easily determined, an empirical control function "EKCF" can be used which exhibits the same behavior as the actual Zeta potential calculated from the data and corrected for surface conduction. EKCF is $-d_B[(E_s/R_c)/\Delta P]$. The floc bed depth d_B, the streaming potential E_s, the floc-filled streaming potential cell resistance R_c and the forcing pressure difference ΔP are all directly determinable in the laboratory. EKCF really involves a streaming current rather than a streaming potential measurement, i.e., $E_s/R_c = I_s$. Direct measurement of I_s was impossible (see Appendix A).

Calculated values of the specific surface conductivity, χ, indicate a decrease in its magnitude with increasing addition of the flocculant PEI. This may indicate replacement of the inorganic ions in the double layer with larger, more

cumbersome and hence less mobile organic PEI cations.

It has been shown, then, that streaming potential data can be used as a better alternate to electrophoretic mobility data for the calculation of an electrokinetic flocculation control parameter. Data obtained on surface conduction's effect on streaming potential measurements should further the present understanding of this phenomenon in that a cationic polyelectrolytic organic adsorbate reduces the specific surface conductivity, χ , for the systems studied.

Further work should include analogous experimental evaluation of a more realistic process, e.g. water containing NaCl as the major electrolyte instead of KCl. Applicability of the "EKCF" function would then be better evaluated. Use of solids other than silica and use of other flocculants might also be considered.

VIII. Conclusions.

1. Zeta potentials have been shown to be useful in determining optimum conditions for the systems studied.
2. Streaming potential data have been shown to be more reliable than electrophoretic data when used for the calculation of a representative Zeta potential.
3. When the bulk properties of the system are used to calculate Zeta potential from streaming potential data, serious errors are encountered at low electrolyte concentrations due to surface conduction phenomena.

4. An electrokinetic control factor calculated from 4 directly measurable quantities, bed depth, streaming potential, forcing pressure and electrolytic resistance of the cell, has been shown to be very reliable. This empirical form is not affected by surface conduction phenomena nor are the inadequacies of an improperly defined Zeta potential involved.
5. Surface conduction as shown by the specific surface conductivity, decreases as the amount of PEI flocculant added increases.

IX. Appendix A

Direct measurement of streaming current, I_s.

If the streaming potential cell is effectively short-circuited by using the electrometer as a zero resistance ammeter, a direct measurement of the streaming current would seem feasible. However, since the values of I_s are in the range of 0 - 3 microamperes, the current flowing across the electrode double layer is 0 - 3 microamperes. This current may be sufficient to cause polarization of the electrodes.

One possible cause for this polarization may be the adsorption of PEI onto the AgCl surface. PEI is an organic molecule and organics have been shown to reduce the capacity of the electrode double layer. A reduction in capacity then increases the effect of polarization (120-121). Another view (122) is that PEI may complex with AgCl and therefore change the nature of the electrode itself so that it is no longer a reversible Ag,AgCl electrode.

Polarization causes a decrease in current flow so that the current I_a reaching the ammeter is less than the streaming current I_s. An apparent DC resistance $R_a = E_s/I_a$, where E_s is the streaming potential and I_a the measured current, would then be greater than the actual resistance $R_c = E_s/I_s$. Data from this laboratory bear this out.

An AC high frequency (1000-3000 cps) measurement of resistance, R_{bridge}, would more likely be close to the true value of R_c, since the high frequency suppresses electrode polarization.

The best way to measure streaming current I_s is then indirectly as E_s/R_c. A measurement of the streaming potential E_s using a high input impedence electrometer (10^{14} ohms e.g.) can be made, followed by an AC high frequency measurement of R_c using a sensitive AC Wheatstone bridge.

X. Nomenclature

A	area perpendicular to current flow, cm^2
A'	constant of Smellie-La Mer eighth power law
A_c	overall cross-sectional area of streaming potential cell, cm^2
A_E	apparent effective area, equal to d_B/K_a, cm^2
A_s	area of double layer capillary annulus perpendicular to current flow, cm^2
abcd	face of area A perpendicular to current flow
B'	constant of Smellie-La Mer eighth power law
C	bulk liquid conductance, mho
C_c	net filled-capillary conductance, mho
C_s	surface conductance, mho
D	dielectric constant
d	particle diameter, cm
d_B	floc bed depth, cm
d_{sv}	surface - volume mean particle diameter, cm
E	potential difference, volt
$dE/d\triangle P$	slope of recorded plot of E_s vs $\triangle P$

E_s	streaming potential, volt
efgh	face of area A perpendicular to current flow
EKCF	empirical electrokinetic control function, equal to $-d_B (E_s/\triangle P)/R_c$
f	frequency
I	current, amp
I_a	current measured by zero resistance ammeter, amp
I_c	return conduction current, amp
I_s	streaming current, amp
K	cell constant, cm^{-1}
K_a	apparent cell constant, equal to λR_c, cm^{-1}
K_s	cell constant of double layer capillary annulus, cm^{-1}
L	capillary length, cm
L'	length between faces abcd and efgh, cm
M	constant, equal to $L/(2\pi r)$
N	normality
n	number of $-CH_2CHNH-$ groups
$\triangle P$	pressure difference
P_m	amount of added flocculant corresponding to maximum refiltration rate

P_o	amount of added flocculant
PEI	polyethyleneimine
Q	refiltration rate
Q'	refiltration rate when $P_o = 0$
R	resistance, ohm
R_a	apparent D.C. resistance, equal to E_s/I_a, ohm
R_{bridge}	resistance of streaming potential cell, measured with high frequency bridge, ohm
R_c	resistance of streaming potential cell, ohm
R_s	resistance which is reciprocal of C_s, ohm
RFR	refiltration rate, ml/min
r	capillary radius, cm
r_H	hydraulic radius, cm
S	area perpendicular to fluid flow, cm^2
s	distance of electrokinetic shear plane from capillary center, cm
s_p	particle surface area, cm^2
U_e	electrophoretic mobility, (cm/sec)/(volt/cm)
u	linear velocity at distance x from capillary center, cm/sec
$\bar{u}$	uniform linear velocity of bulk liquid, cm/sec

v_p	particle volume, cm^3
x	distance from capillary center, cm
y	distance in liquid phase measured from solid-liquid interface
ZPA	apparent Zeta potential, calculated on basis of bulk liquid specific conductivity, volt
ZPC	Zeta potential, corrected for effect of surface conduction, volt
δ	thickness of mobile part of liquid side of double layer, cm
δ'	thickness of condenser used in Helmholtz double layer model
ϵ	porosity
ζ	zeta potential; potential difference between electrokinetic shear plane and bulk liquid, volt
ζ_T	corrected Zeta potential, based on methid of Oulman and Baumann
η	liquid viscosity
λ	bulk liquid specific conductivity, mho.cm
λ_c	capillary effective liquid specific conductivity, mho/cm
λ_s	specific conductivity of liquid in double layer capillary annulus, mho/cm
ξ	electric field intensity; potential gradient, volt/cm

ρ	volumetric charge density, coulombs/cm^3
σ	net surface charge density, coulombs/cm^2
ϕ	Galvani potential difference between bulk solid and bulk liquid phases, volt
χ	specific surface conductivity, (cm ·mho/cm) or mho
$\bar{\psi}$	potential with respect to bulk liquid phase, volt
ψ_1	potential difference between bulk liquid phase and plane separating inner and outer Stern layers, volt
Ω	wetted perimeter perpendicular to fluid flow, cm

XI. References.

1. La Mer, V. K and Smellie, R. H. Jr., J. Colloid Sci., 11, 704-709 (1956).

2. La Mer, V. K., and Smellie, R. H. Jr., J. Colloid Sci., 11, 710-719 (1956).

3. Smellie, R. H., Jr., and La Mer, V. K., J. Colloid Sci., 11, 720-731 (1956).

4. La Mer, V. K., Smellie, R. H. Jr., and Lee, P. K., J. Colloid Sci., 12, 230-239 (1957).

5. La Mer, V. K., Smellie, R. H., Jr., and Lee, P. K., J. Colloid Sci., 12, 566-574 (1957).

6. Smellie, R. H., Jr. and La Mer, V. K., J. Colloid Sci., 13, 589-599 (1958).

7. Healy, T. W., and La Mer, V. K., J. Phys. Chem., 66, 1835 (1962).

8. Dixon, J. K., La Mer, V. K., Li, C., Messinger, S., and Linford, H. B., J. Colloid and Interface Sci., 23, 465-473 (1967).

9. Linford, H. B., Li, C., and Messinger, S., U.S. Public Health Service Terminal Progress Report, WP00240-05, (1967).

10. Dixon, J. K., La Mer, V. K., Li, C., Messinger, S., and Linford, H. B., J. Colloid and Interface Sci., 23, 465-473 (1967).

11. Ockershausen, R. W., and Peterman, C. K., J. Am. Water Works Assoc., 56, 2, 224 (1964).

12. Baker, R. A., Campbell, S. J. and Anspach, F. R., J. Am. Water Works Assoc., 57, 3, 363 (1965).

13. Linford, H. B., Li, C., and Messinger, S., US Public Health Service Terminal Progress Report, WP00240-05 (1967).

14. Ibid.

15. Ibid.

16. Briggs, D. R., J. Phys. Chem., 32, 641 (1928).

17. Joly, M., J. Colloid Sci., 11, 519 (1956).

18. Grahame, D. C., J. Chem. Phys., 18, 903 (1950).

19. Saline Water Conversion Report, 1965, U.S. Department of the Interior, Office of Saline Water, p. 145.

20. Iler, R. K., Colloid Chem. of Silica and Silicates, Cornell Univ. Press, Ithaca, N.Y., 1955, Chapters 7 and 8.

21. La Mer, V. K., J. Colloid Sci., 19, 291-293 (1964).

22. La Mer, V. K., and Smellie, R. H., Jr., J. Colloid Sci. 11, 704-709 (1956).

23. La Mer, V.K., and Smellie, R. H., Jr., J. Colloid Sci., 11, 710-719 (1956).

24. Smellie, R. H., Jr. and La Mer, V. K., J. Colloid Sci., 11, 720-731, (1956).

25. La Mer, V. K., Smellie, R. H., Jr. and Lee, P. K., J. Colloid Sci., 12, 230-239 (1957).

26. La Mer, V. K., Smellie, R. H., Jr., and Lee, P. K., J. Colloid Science, 12, 566-574 (1957).

27. Smellie, R. H., Jr. and La Mer, V. K., J. Colloid Sci., 13, 589-599 (1958).

28. Healy, T. W. and La Mer, V. K., J. Phys. Chem., 66, 1835 (1962).

29. Kane, J. C., La Mer, V. K., and Linford, H. B. J. Phys. Chem. 67, 1977 (1963).

30. Kane, J. C., La Mer. V. K., and Linford, H. B., J. Am. Chem. Soc., 86, 3450 (1964).

31. Gaudin, A. M., and Fuerstenau, D. W., Mining Engineering, 7, 1, (1955).

32. Kane, J. C., La Mer, V. K., and Linford, H. B., J. Am. Chem. Soc., 86, 3450 (1964).

33. Healy, R. W., J. Colloid Sci., 16, 609-617 (1961).

34. Dixon, J. K., La Mer, V. K., Li, C., Messinger, S., and Linford, H. B., J. Colloid and Interface Sci., 23, 465-473 (1967).

35. Linford, H. B., Li, C., and Messinger, S., U.S. Public Health Service Terminal Progress Report, WP00240-05 (1967).

36. J. Phys. Chem., 67, 1980-1981 (1963).

37. Kane, J. C., La Mer, V. K., and Linford, H. B., J. Phys. Chem., 68, 3539 (1964).

38. Linford, H. B., Li, C., and Messinger, S., U.S. Public Health Service Terminal Progress Report, WP00240-05 (1967).

39. Ibid.

40. Ockershausen, R. W., and Peterman, C. K., J. Am. Water Works Assoc., 56, 2, 224 (1964).

41. Baker, R. A., Campbell, S. J., and Anspach, F. R., J. Am. Water Works Assoc., 57, 3, 363, (1965).

42. Dixon, J. K., La Mer, V. K., Li, C., Messinger, S., and Linford, H.B., J. Colloid and Interface Sci., 23, 465-473 (1967).

43. Linford, H. B., La Mer, V. K., Li, C. and Messinger, S., U.S. Public Health Terminal Progress Report WP00240-04 (1966).

44. Ibid.

45. Fyfe, R. R., Master's Thesis, Columbia University, (1966).

46. Dixon, J. K., La Mer, V. K., Li, C., Messinger, S. and Linford, H. B., J. Colloid and Interface Sci., 23, 465-473 (1967).

47. Linford, H. B., Li, C., and Messinger, S., U.S. Public Health Service Terminal Progress Report, WP0024C-05 (1967).

48. Zeta-Meter, Inc., New York, N.Y.

49. Ockershausen, R. W., and Peterman, C. K., J. Am. Water Works, Assoc., 56, 2, p224 (1964).

50. Baker, R. A., Campbell, S. J., and Anspach, F. R., J. Am. Water Works Assoc., 57, 3, p363 (1965).

51. Linford, H. B., Li, C., and Messinger, S., U.S. Public Health Service Terminal Progress Report, WP00240-05 (1967).

52. Joly, M., J. Colloid Sci., 11, 519 (1956).

53. Grahame, D. C., J. Chem. Phys. 18, 903 (1950).

54. Kruyt, H. R., Editor, Colloid Science, Vol. 1, Elsevier Publishing Co., New York, 1952, pp 206-237.

55. Briggs, D. R., J. Phys. Chem. 32, 641 (1928).

56. Rutgers, A. J., Trans, Faraday Soc., 36, 69 (1940)

57. Kruyt, H. R., editor, Colloid Science, Vol. 1, Elsevier Publishing Co., New York, 1952, pp 206-237.

58. Hampel, C. A., editor, The Encyclopedia of Electrochemistry, Reinhold Publishing Corp., New York, 1964, pp.1088, 1090 and 471-475.

59. Rutgers, A. J., Transactions of the Faraday Society, 36, 69 (1940).

60. Orr, C., Jr. and Dallavalle, J. M., Fine Particle Measurement, MacMillan, New York, 1959, Chapters 2 and 6.

61. Zucker, G. L., Doctoral Dissertation, Columbia University, (1959).

62. Briggs, D. R., J. Phys. Chem. 32, 641 (1928).

63. Oulman, C. S., and Baumann, E. R., J. Am. Water Works Assoc. 56, 7, p.915 (1964).

64. Kruyt, H.R., Editor, Colloid Science, v. 1., Elsevier Publishing Co., New York 1952, p.206-237.

65. Glasstone, S., An Introduction to Electrochemistry, Van Nostrand Co., Inc., New York, 1942, Chapter XVI.

66. Kruyt, H. R., Editor, Colloid Science, V.1, Elsevier Publishing Co., New York, 1952, pp. 206-237.

67. Culman, C. S., and Baumann, E. R., J. Am. Water Works Assoc. 56, 7, p.915 (1964).

68. Kruyt, H. R., Editor, Colloid Science, v.1, Elsevier Publishing Co., New York, 1952, p. 206-237.

69. Briggs, D. R., J. Phys. Chem. 32, 641 (1928).

70. Rutgers, A. J., Transactions Faraday Soc., 36, 69 (1940).

71. Oulman, C. S., and Baumann, E. R., J. Am. Water Works Assoc. 56, 7, p.915 (1964).

72. Rutgers, A. J., and DeSmet, M., Trans. Faraday Soc., 43, 102 (1947).

73. White, H. L., Monaghan, B., and Urban, F., J. Phys. Chem. 40, 207 (1936).

74. Ibid.

75. Hampel, C. A., editor, The Encyclopedia of Electrochemistry, Rheinhold Publishing Corp. New York, 1964, p.1088, 1090.

76. Ives, D. J. G. and Janz, G. J. Reference Electrodes Theory and Practice, Academic Press, New York, 1961, Chapter 4.

77. Falk, G., and Lange, E., Z. Elecktrochem., 54, 133 (1950).

78. Karasyk, L., and Linford, H. B., J. Electrochem. Soc., 110, 895-904 (1963).

79. Iler, R. K., The Colloid Chemistry of Silica and Silicates, Cornell University Press, Ithaca, New York, 1955, Chapters 7 and 8.

80. Iler, R. K., The Colloid Chemistry of Silica and Silicates, Cornell University Press, Ithaca, New York, 1955, Chapters 7 and 8.

81. Ibid.

82. Dixon, J. K., La Mer, V. K., Li, C., Messinger, S., and Linford, H. B., J. Colloid and Interface Sci., 23, 465-473 (1967).

83. Glasstone, S., An Introduction to Electrochemistry, Van Nostrand Co., Inc., New York, 1942, Chapter XVI.

84. Hampel, C. A., editor, The Encyclopedia of Electrochemistry, Reinhold Publishing Corp., New York, 1964, p.471

85. Glasstone, S., An Introduction to Electrochemistry, Van Nostrand Co., Inc., New York, 1942, Chapter XVI.

86. Ibid.

87. Ibid.

88. Ibid.

89. Delahay, P., Double Layer and Electrode Kinetics, Interscience Publishers, New York, 1966, Chapter 3.

90. Glasstone, S., An Introduction to Electrochemistry, Van Nostrand Co., Inc., New York 1942, Chapter XVI.

91. Ibid.

92. Dixon, J. K., La Mer, V. K., Li, C., Messinger, S., and Linford, H. B., J. Colloid and Interface Sci., 23, 465-473 (1967).

93. Hampel, C. A., editor, The Encyclopedia of Electrochemistry, Reinhold Publishing Corp., New York, 1964, pp. 1088, 1090.

94. Glasstone, S., An Introduction to Electrochemistry, Van Nostrand Co., Inc., New York, 1942, Chapter XVI.

95. Joly, M., J. Colloid Sci., 11, 519 (1956).

96. Grahame, D. C., J. Chem. Phys., 18, 903 (1950).

97. Briggs, D. R., J. Phys. Chem. 32, 641 (1928).

98. Ibid.

99. Rutgers, A. J., Transactions Faraday Soc., 36, 69 (1940).

100. Oulman, C. S., and Baumann, E. R., J. Am. Water Waorks Assoc., 56, 7, p.915 (1964).

101. Rutgers, A. J., and De Smet, M., Trans. Faraday Soc., 43, 102 (1947).

102. White, H. L., Monaghan, B., and Urban, F., J. Phys. Chem. 40, 207 (1936).

103. Orr, C., Jr. and Dallavalle, J. M., Fine Particle Measurement, MacMillan, New York, 1959, Chapters 2 and 6.

104. Ibid.

105. Kane, J. C., La Mer, V. K., and Linford, H. B., J. Phys. Chem. 67, 1977 (1963).

106. Martin, W. McK., and Gortner, R. A., J. Phys. Chem. 34, 1509 (1930).

107. Loomis, G. A., J. Am. Ceramic Soc., 21, 393 (1938).

108. Li, C., Master's Thesis, Columbia University (1967).

109. Private communication with Linford, H. B., Columbia University.

110. Loomis, G. A., J. Am. Ceramic Soc., 2, 393 (1938).

111. Ibid.

112. Orr, C., Jr. and Dallavalle, J. M., Fine Particle Measurement, MacMillan, New York, 1959, Chapters 2 and 6.

113. Kruyt, H. R., editor, Colloid Science, Vol. 1, Elsevier Publishing Co., New York, 1952, p. 237.

114. Dixon, J. K., La Mer, V. K., Li, C., Messinger, S., and Linford, H. B., J. Colloid and Interface Sci., 23, 465-473 (1967).

115. Glasstone, S., An Introduction to Electrochemistry, Van Nostrand Co., New York, 1942, Chapter XVI.

116. Briggs, D. R., J. Phys. Chem., 32, 641 (1928).

117. Rutgers, A. J., Trans. Faraday Soc., 36, 69 (1940).

118. Rutgers, A. J., and De Smet, M., Trans. Faraday Soc., 43, 102 (1947).

119. White, H. L., Monaghan, B., and Urban, F., J. Phys. Chem., 40, 207 (1936).

120. Falk, G., and Lange, E., Z. Elecktrochem., 54, 133 (1950).

121. Karasyk, L., and Linford, H. B., J. Electrochem. Soc., 110, 895-904 (1963).

122. Sager, T.M.H., Doctoral Thesis, Polytechnic Institute of Brooklyn, June 1965.

XII. Index of Figures and Tables.

Figure		Page
1	x - y diagram	26
2	Streaming potential capillary	31
3	Conductivity cube	36
4	Alternate conduction paths	40
5	Streaming potential cell	48
6	Ag,AgCl electrode	50
7	Assembly of streaming potential cell	53
8	Streaming potential apparatus	55
9	Streaming potential apparatus with conductivity cell attached	57
10	Andreasen pipette	61
11	Large settling pipette with enclosure	63
12	Filtration and refiltration apparatus	68
13	Refiltration apparatus using buret as filtrate supply	70
14	RFR vs. PPM PEI for 0.4 wt% silica	81
15	d_{sv} vs. PPM PEI for 0.4 wt% silica	83
16	ZPA vs. PPM PEI for 0.4 wt% silica	85
17	EKCF vs. PPM PEI for 0.4 wt% silica	88
18	A_E vs. PPM PEI for 0.4 wt% silica	90
19	ZPC vs. PPM PEI for 0.4 wt% silica	93
20	"X" vs. PPM PEI for 0.4 wt% silica	96
21	Correlations for 0.4 st% silica	100

Table		
1	Flocculation systems matrix	66
2	Tabulation of results	75
3		98